2016-02-04

Effect of Downhole Vibration on Coiled Tubing Reach in Horizontal Intervention

Yekta Ganjeh, Kaveh

UNIVERSITY OF CALGARY

Effect of Downhole Vibration on Coiled Tubing Reach in Horizontal Intervention

by

Kaveh Yekta Ganjeh

A THESIS

SUBMITTED TO THE FACULTY OF GRADUATE STUDIES

IN PARTIAL FULFILMENT OF THE REQUIREMENTS FOR THE

DEGREE OF MASTER OF SCIENCE

GRADUATE PROGRAM IN MECHANICAL ENGINEERING

CALGARY, ALBERTA

FEBRUARY, 2016

Abstract

Technological advances enabled horizontal drilling to expose deeper and longer horizontal lateral sections, thereby maximizing producing zones in reservoirs. The use of Coiled Tubing (CT) to perform different types of well intervention operations is limited by the maximum depth in the horizontal section. One of the most effective remedies is the application of downhole vibration. This thesis proposes a method to describe the effect of vibrations to improve load transfer for a CT with a straight, a sinusoidally buckled and a helically buckled configuration. In order to capture the effect of vibration on the reduction of friction, the concept of apparent friction factor is introduced for all three types of section. The proposed approach is validated against published experimental data, for both the non-vibrating and the vibrating cases. Full wellbore axial force transfer and slack-off weight models are developed to simulate the effect of downhole vibration to enhance CT reach.

Acknowledgements

I would like to thank Dr. Les Sudak for having been my supervisor and for his support through these years.

I would like to express my most wholehearted thanks to Dr. Salvatore Federico for his supervision, unlimited support and friendship throughout this work. Dr. Federico was my initial supervisor and later, for bureaucratic reasons, became my co-supervisor. He provided me with his support and guidance in every step of this work, and especially in the last few months prior to my graduation. Dr. Federico provided me with a lot of technical feedback on my research project and helped me to prepare a professionally written thesis. Whenever there was a challenge for me to face during this work, Dr. Federico was there to offer his advice and support.

I would like to thank Dr. Marcelo Epstein for recommending me to Dr. Federico to start my MSc program under Dr. Federico's supervision as well as for serving in my examining committee. His questions during the exam and his support after the exam undoubtedly brought me confidence that I had done the job right.

I would like to thank Dr. Hussein Hejazi for serving in my examining committee, for his careful reading of my work, and for his valuable feedback during the examination.

I would like to thank Dr. Meera Singh for serving in my examining committee.

Dedication

To my lovely wife, Azadeh, for her constant and unconditional support, patience, encouragement and sacrifice throughout this work. Without her, I would not have been able to finish this work.

To our beautiful and lovely little girl, Elena, who is the source of love and happiness in our life.

To my late mom and dad, who are not with us to see their son’s achievement. God bless them.

Table of Contents

Abstract ii
Acknowledgements iii
Dedication iv
Table of Contents v
List of Figures and Illustrations vii

Chapter 1. Introduction 1

Chapter 2. Literature Review 5

Chapter 3. Coiled Tubing Services 17

3.1. Coiled Tubing Equipment 19
3.1.1. Coiled Tubing String 19
3.1.2. Coiled Tubing power pack unit 20
3.1.3. Coiled Tubing Control Cabin 21
3.1.4. Coiled Tubing Reel 23
3.1.5. Coiled Tubing Injector Head and Gooseneck 25
3.1.6. Stripper (Stuffing Box) 27
3.1.7. Blowout Preventer (BOP) 28
3.1.8. Downhole Tools 30

3.2. Coiled Tubing Applications 32
3.2.1. Coiled Tubing Cleanout 32
3.2.2. Coiled Tubing Milling 33
3.2.3. Coiled Tubing Logging 33
3.2.4. Coiled Tubing Matrix Stimulation (Acidizing) 34
3.2.5. Coiled Tubing Drilling 34
3.2.6. Coiled Tubing Fracturing 35
3.2.7. Coiled Tubing Cementing 35
3.2.8. Coiled Tubing Fishing 36
3.2.9. Coiled Tubing Nitrogen Kick off 36
3.2.10. Application of Coiled Tubing Equipped with Optical Fibers 37

3.3. Job Design Considerations for Coiled Tubing Services 37

3.4. Downhole Vibrating Tool 38

Chapter 4. Theoretical Background 41

Chapter 5. Modeling 61

5.1. Modeling vs Published Experimental Data 61

5.2. Full Wellbore Modeling 68

Chapter 6. Summary and Recommendations 83

References 85
Appendix A Force-Pitch Relationship 93
Appendix B Sinusoidal Buckling Load 96
Appendix C Helical Buckling Load 98

List of Figures and Illustrations

Figure 3-1: Coiled Tubing equipment rig-up configuration 18

Figure 3-2: Power pack skid unit 21

Figure 3-3: Coiled Tubing control unit 23

Figure 3-4: Coiled Tubing Reel unit 25

Figure 3-5: Coiled Tubing injector head and Gooseneck 27

Figure 3-6: Coiled Tubing Stripper (Stuffing Box) 28

Figure 3-7: Coiled Tubing Blowout Preventer (BOP) 30

Figure 3-8: Downhole Bottom Hole Assembly (BHA) – (Bakke Oil Tools Catalog 2001) 32

Figure 3-9: Downhole vibrating tool (Agitator) 40

Figure 4-1:Buckling of string in wellbore 42

Figure 4-2:Helix geometry and pitch of buckled string 44

Figure 4-3: Configuration of string in wellbore 47

Figure 4-4: Sinusoidal buckled string in horizontal wellbore 51

Figure 4-5: Helical buckled string in horizontal wellbore 52

Figure 4-6: Force balanced in horizontal wellbore 53

Figure 4-7: Lock-up condition graph 59

Figure 5-1: Experimental data extracted from Wu and Juvkam-Wold (1993c) 62

Figure 5-3: Experimental data extracted from Newman et al. 64

Figure 5-4: Axial loading vs Experimental data for non-vibrating case 65

Figure 5-7: Axial Loading Models for Vibrating and Non-Vibrating Cases 68

Figure 5-10: Wellbore survey in 2D 71

Figure 5-11: Wellbore Completions 72

Figure 5-14: Slack off weight calculation for vertical and curved (heel) sections 75

Figure 5-15: Slack off weight calculation for vertical, curved and horizontal sections 76

Figure 5-16: Axial Compressive force for CT string at depth of 4584.91 mMD 77

Figure 5-17: Slack off weight graph for CT string at depth of 4584.91 mMD..... 78

Figure 5-18: Axial Compressive force for CT string at depth of 4665.92 mMD 79

Figure 5-19: Slack off weight graph for CT string at depth of 4665.92 mMD..... 80

Figure 5-20: Downhole Vibration Application - Axial Compressive force at 4665.92 mMD 81

Figure 5-21: Downhole Vibration Application – Slack off weight at 4665.92 mMD 82

Chapter 1. Introduction

Coiled Tubing (CT) is a very long and continuously milled pipe which is manufactured in different sizes and lengths. Coiled Tubing pipes, along with different surface equipment and downhole tools, are used for intervention operations in the oil and gas industry. Coiled Tubing surface equipment consists of power pack, control cabin, reel (spool), Gooseneck (arch guide), injector, stripper and blowout preventer (BOP). Selected sets of downhole tools suitable for intervention purpose are conveyed with the Coiled Tubing string. Coiled Tubing services is the collective name of the application of Coiled Tubing string, surface equipment and downhole tools to perform different well intervention and well serving operations. Coiled Tubing has different applications such as CT cleanout, milling, logging, matrix stimulation (acidizing), drilling, fracturing cementing, fishing and nitrogen kick-off. The possibility of deployment in horizontal wells and of pumping fluid/nitrogen are among the main advantages of Coiled Tubing services compare to other intervention methods such as Wire-line and Slick-line services.

The main challenges in horizontal intervention are reaching to desired depth and providing proper weight on bit (WOB), intended as the force to be exerted on downhole tool to perform the desired operation. The friction force between the wellbore and the CT string increases as the horizontal section gets more extended. An increase in this wellbore drag causes some sections of the CT string to buckle into a sinusoidal configuration and subsequently into a helical configuration. Once the CT has buckled into the helical shape, the wellbore friction increases significantly and the CT cannot be pushed farther into the wellbore causing to “lock-

up". One of the solutions to this problem is the introduction of downhole vibration. The downhole vibrating tool is a component of the bottomhole assembly (BHA) that is used to create axial vibration at the bottom section of the CT string. The downhole vibrating tool provides axial vibration as a result of the fluid pumped into the tool through the CT. Downhole vibration enables CT string to extend its reach in a wellbore that was initially restricted due to the lock-up condition.

The buckling phenomenon in a drilling string and in a CT string has been studied extensively by various researchers. Early studies focused on buckling in various completion configurations in the wellbore. Several studies have aimed at understanding sinusoidal and helical buckling effects in a drill string and in a CT string.

Many different aspects of buckling in drilling and well intervention have been studied both experimentally and theoretically. For instance, models have been developed for the force transfer relationship in vertical, deviated and horizontal wellbore, the effect of friction, variable pitch, wellbore curvature, lock-up condition, contact force due to sinusoidal/helical buckling, torque and shear. Soft string modeling is used to calculate the axial force in the CT string and stiff string (beam-column) modeling is used to model the long BHA used in drilling applications.

On the contrary, there are not as many studies regarding the effect of downhole vibration in CT application. The proprietary nature of such modeling could be one the reasons: the companies that develop them do not reveal most details.

Newman et al. (2007a, 2007b and 2009) conducted surface tests in order to investigate the effect of vibration and rotation on reducing the friction. It was mentioned that a model was

developed to analyze the effect of vibration on load transfer but the details of the model were not revealed in their studies.

In order to model the reach of the CT string to a certain depth using a downhole vibration tool, it is required to understand the effect of vibration on the enhancement of load transfer from the surface to downhole and on the reduction of wellbore friction drag.

The present study proposes a modeling method to describe the effect of vibrations on improving load transfer using straight, sinusoidal and helical buckling configurations. Additionally, the study uses an application of apparent friction factor concept for all three sections as a means to capture the effect of vibration to reduce friction. The proposed approach is validated against published experimental data, for both the non-vibrating and the vibrating cases. Full wellbore axial force transfer and slack-off weight models are developed in order to simulate the effect of downhole vibration to enhance CT reach. Axial load transfer simulations are run for the entire wellbore with and without the application of downhole vibrating tool. The improvement in CT reach achieved by the application of downhole tools is verified by means of numerical simulations.

This thesis is structured as follows. Chapter 2 provides a summary of the research about different aspects of the buckling phenomenon and the effect of downhole vibration in the oil and gas industry. Chapter 3 consists of four sections: Section 3.1 (Coiled Tubing Equipment) reviews different components which are used in every CT operation and explains their function; Section 3.2 (Coiled Tubing Application) explains different services which are used in intervention operations; Section 3.3 (Job Design Considerations) outlines the requirements for

modeling an intervention job using CT services and the limitations arising at the modeling stage; Section 3.4 (Downhole Vibrating Tool) reviews the different components and function of this type of downhole tool. Chapter 4 reports published criteria for the buckling of CT string and the use of energy methods to derive the relationship for sinusoidal and helical buckling. The axial load distribution force relationship for vertical, curved and horizontal section of wellbore are derived. The governing differential equations that are used to calculate the axial load force for different sections of well are also presented. Chapter 5 is the work developed in this thesis, and presents experimental tests and data from the literature and proposes a modeling approach to explain the effect of downhole vibration to enhance load transfer using such data. A full wellbore axial load distribution and slack off weight (lock-up condition) simulations are presented for both non-vibrating and vibrating cases. Finally, Chapter 6 presents a summary of the results of this thesis and outlines the possible future work.

Chapter 2. Literature Review

The buckling of a pipe in a wellbore has been studied for many years in the oil and gas industry. In the early stages of this study, the focus was on drilling and completions (packers) applications and, subsequently, on coiled tubing as well as intervention applications. Lubinski (1950) studied the theory of buckling of rotary drill string in one plane. Lubinski et al. (1962) presented the effect of helical buckling in packer-tubing system for several different configurations. The pitch-force relationship for helically buckled tubing was derived, based on energy methods, as (see Appendix A.)

$$F = \frac{8\pi^2 EI}{p^2}, \tag{2.1}$$

where F is compressive force along the axis of the helix, E is Young's modulus, I is moment of inertia of the cross section and p is pitch of the helix. Paslay and Bogy (1964) studied the stability of the rod in a constrained cylindrical geometry by using energy methods. In their approach, it was assumed that rod maintained constant contact with the circular wellbore, that the angular displacement at the boundary was zero and that no change occurred in the curvature of the tubing. The total potential energy of the system was calculated and minimized in order to find the critical buckling load (F_{crit}).

Walker and Friedman (1977) presented a three-dimensional force and deflection model for studying the drill string. By using the general theory of bending and twisting of rods (e.g., Love, 1944), they presented a mathematical model to calculate force/moment and deflection for

the bottom-hole assembly in a wellbore. Their formulation was based on other researchers' work in beam equilibrium approach, aimed at describing buckling phenomena in a wellbore. Hammerlindl (1980) extended the study on force transmission in packer/tubing system started by Lubinski et al. (1962), and examined the displacements and forces in two-packer configurations for several cases. Mitchell (1982) studied helical buckling in a packer-tubing configuration by using equilibrium equations, and based his study on the drill string deflection analysis presented by Walker and Friedman (1977).

Mitchell (1982) presented a formulation to evaluate stress and deformation at the packer, and considered the influence of the packer and the weightlessness of the tubing. Dawson and Paslay (1984) determined the conditions for the stability of the drill pipe in an inclined well. They used the stability conditions for a circular rod inside a horizontal wellbore, which had been studied by Paslay and Bogy (1964), and obtained the relation

$$F_{crit} = \frac{(1-\upsilon)^2}{(1+\upsilon)(1-2\upsilon)} EI \frac{\pi^2}{L^2}\left(n^2 + \frac{L^4 \rho A g}{n^2 \pi^4 EIr} \right), \qquad (2.2)$$

where F_{crit} is the critical axial load to initiate buckling, υ is the Poisson's ratio, E is Young's modulus, I is cross-section moment of inertia, n is order of buckling, L is length of the drill pipe, ρ is mass density of the pipe, A is the cross-section of the pipe, g is the gravitational force per unit mass, and r is the radial clearance between pipe and wellbore. The formula is for horizontal applications only. Dawson and Paslay (1984) generalized the stability criteria from the horizontal to the inclined wellbore by considering the component of the weight per unit length in

the inclined wellbore ($\rho Ag\sin\theta$). The stability criterion for the inclined wellbore was thus obtained as

$$F_{crit} = EI\frac{\pi^2}{L^2}\left(n^2 + \frac{L^4\rho Ag\sin\theta}{n^2\pi^4 EIr}\right). \tag{2.3}$$

The minimum value of F_{crit} for an inclined wellbore with respect to n resulted in sinusoidal (critical) buckling load as follows (see Appendix B. Equation B-9)

:

$$F_{crit} = 2\sqrt{\frac{EI\rho Ag\sin\theta}{r}}, \tag{2.4}$$

where θ is inclination angle. Dawson and Paslay (1984) also showed that, in a highly inclined hole, the drill pipe is capable of carrying high compressive loads without buckling.

Cheatham and Pattillo (1984) presented a new force-pitch relationship in the extension of the work by Lubinski et al. (1962) for a straight weightless column. They studied the loading and unloading scenario in terms of force-pitch relationship. Mitchell (1986a) used a numerical technique to solve the buckling problem in a tubing/packer configuration and introduced the novel concept of "neutral point" based on the contact force. Mitchell (1986b) also studied the effect of friction in helical buckling phenomena in a vertical wellbore. He studied two simple cases of tubing moving upward and downward: considering the effect of friction, he proposed an axial load distribution for a vertical wellbore with a helically buckled pipe. Sorenson and Cheatham (1986) studied the effect of boundary conditions on the post-buckling configuration of a pipe in a confined circular cylinder, including the contact between the pipe and the wellbore

constraint. A semi-analytical solution for the helical buckling problem was proposed by Kwon (1988), who considered the weight of the pipe and a variable pitch, using a beam-column method (rather than an energy method). The solution proposed by Kwon (1988) was applied to a tapered tubing configuration and solved numerically.

Mitchell (1988) introduced a new approach to solve the helical buckling problem for a tubing/packer completion in a vertical wellbore. He considered the boundary conditions on the packer, a variable helix pitch and tapered completion configurations. Chen et al. (1989) studied the buckling phenomenon in casing/tubing configurations and presented buckling force criteria for sinusoidal and helical buckling in a horizontal wellbore. They derived a sinusoidal buckling load similar to that by Dawson and Paslay (1984) and determined that an increase in the compressive axial load causes the tubing to have a transition from sinusoidal to helical buckling. Chen et al. (1989) applied energy methods to calculate the required criteria for the helically buckling force. Minimization the total energy with respect to the number of full waves in a long horizontal pipe resulted in the expression (see Appendix C for details)

$$F^* = \left(2\sqrt{2}\right)\sqrt{\frac{EIw}{r}}, \tag{2.5}$$

where F^* (also known as F_{hel}) is helical buckling load and w is weight per unit length of the pipe. Chen et al. (1989) also conducted experiments in order to verify the validity of their proposed relationship. Zhang (1989) considered variable pitch in the study of a helically buckled drill string in a vertical wellbore: the variable helix pitch was deemed to be beneficial to the

calculation of the drill string configuration. He assumed that the friction force is reduced and does not have any effect on the stability of the drill string because of axial vibration.

In a different publication, Chen et al. (1990) again presented sinusoidal and helical buckling criteria for a pipe in a horizontal wellbore and performed experiment to support their findings. Chen and Adnan (1993) studied the effect of gravity on helical buckling in an inclined wellbore, by means of energy methods. Wu and Juvkam-Wold (1993a, 1993b) improved the calculation of the helical buckling load by implementing a linearly increasing axial force under buckling, instead of a constant one. The new helical buckling load F_{hel}, based on energy methods, is

$$F_{hel} = 2\left(2\sqrt{2}-1\right)\sqrt{\frac{EIw\sin\theta}{r}}\,. \tag{2.6}$$

Wu and Juvkam-Wold (1993a, 1993b) also performed experimental tests to verify their proposed relationship for the helical buckling load, and (1993c) introduced axial load distribution in inclined and horizontal wellbore due to the helical buckling effect. In a test simulating a horizontal wellbore, the input and output forces were measured while the specimen was in helical buckling mode. The evaluated axial load distribution was in a good agreement with the experimental results. Gu et al. (1993) studied force transmission in CT operations, and introduced a method to calculate slack off weight in vertical and inclined wellbore. A belt friction model was used to describe force transmission and contact force in a curved wellbore with constant curvature. McCann and Suryanarayana (1994) performed extensive experimental tests to study the effect of curvature and friction on helical buckling. In their experimental tests,

they observed that snapping and reverse snapping, which are instabilities due to friction, can be reduced by introducing vibration. Salies et al. (1994a) performed experimental tests in helical buckling and compared the results with a Finite Element model. Bhalla (1994) developed a tubing force model for a CT string considering an initial residual bend and its effect on force transmission, and also proposed the application of a single friction coefficient for loading (Run In Hole, RIH) and unloading (Pull Out Of Hole, POOH). He validated his proposed relationship against field data.

We would like to remark that soft string modeling is used in Coiled Tubing application in order to calculate the axial force in the full wellbore. The string is divided into distinct deformable elements to form a chain (or rope). It is assumed that:

1. the axial forces are supported by the CT string and the lateral contact forces are supported by the wellbore;
2. the CT string deforms to the shape of wellbore and maintains constant contact with wellbore.

On the other hand, stiff string modeling considers bending of the CT, which is more applicable in drilling application with:

1. long BHA in 3 dimensional surveys;
2. sharp changes of azimuthal angle.

In this scenario, using the stiff string assumption to account for the effects of bending on the BHA produces more accurate results. We also mention that, normally, stiff string modeling is usually coupled with a Finite Element analysis. In this thesis, no azimuthal change is considered, so that the axis of the wellbore is entirely contained in a vertical plane. For this reason, soft string

modeling is considered suitable to show the effect of downhole vibration in a full wellbore and for the calculation of the axial forces.

Experimental tests were conducted by Salies et al. (1994b) to study sinusoidal bucking in a vertical wellbore. He and Kyllingstad (1995) modeled the effect of wellbore curvature on helical buckling load, and demonstrated that the model including the curvature of the wellbore gives a less conservative criterion for helical buckling. Two different post-buckling criteria were proposed for CT operations envelope: lock-up and failure due to excess of axial and bending stress (or F_y-Yield force). He and Kyllingstad (1995) defined the lock-up condition quantitatively as

$$\frac{\Delta F_{out}}{\Delta F_{in}} \approx 0\,, \tag{2.7}$$

where F_{out} is the downhole force and F_{In} is the slack off weight (surface weight).

For numerical calculations, condition (2.7) be stated as

$$\frac{\Delta F_{out}}{\Delta F_{in}} < 0.01\,. \tag{2.8}$$

They also showed that the tubing may fail due to exceeding the yield stress, which can occur before the lock-up condition.

Miska and Cunha (1995) studied the effect of torque on helical buckling load in inclined wellbore and neglected the effect of friction. Mitchell (1995) presented the pull-through force for downhole tools in the wellbore using contact force and friction. Wu (1995) showed that considering the contact force resulting from sinusoidal buckling had an impact on helical

buckling and the compressive axial load distribution. He also presented a new sinusoidal contact force model, as well as a calculation of the axial force distribution in a horizontal wellbore due to the effect of sinusoildal buckling. Wu and Juvkam-Wold (1995a) performed a comprehensive analysis of force transmission for different sizes of CT strings and proposed new equations to predict the buckling of a string. The new helical buckling load for a vertical wellbore was proposed as

$$F_{hel,b} = 5.55\left(EIW_e^{\,2}\right)^{1/3}, \tag{2.9}$$

where $F_{hel,b}$ is helical buckling load in the vertical wellbore, E is the Young's modulus, I is the cross-sectional moment of inertia and W_e is the tubular weight in mud. In continuation of their previous works, Wu and Juvkam-Wold (1995b) studied sinusoidal and helical buckling of a string in an inclined wellbore, and considered the effect of the tubular weight component on sinusoidal and helical buckling load. Wu and Juvkam-Wold (1995c) developed relationships for curvature-dependent sinusoidal and helical buckling loads, and compared their new method with previously published criteria.

The effect of friction in the helical buckling of a tubular string in production and stimulation operations was studied by Mitchell (1996) using the Finite Element Method (FEM). In his model, a displacement-based approach was used rather than a force calculation. Akgun et al. (1996) used FEM along with experiments to study the drill string behavior. Miska et al. (1996) presented improved modeling for force transfer for the case of straight, inclined and horizontal wellbores, and compared their results with experimental data. They claim that their

axial force transfer model for the sinusoidal case is introduced for the first time. For the axial force model, they assumed that the CT is deformed into a helical shape. Hishida et al. (1996) performed experiment with a straight pipe specimen in a vertical position under sinusoidal and helical buckling configurations. The effect of contact force between the specimen pipe and outer pipe was not considered. They also developed a FEM model using beam elements, in order to predict buckling deformation and for comparison with their experimental work. Qiu et al. (1997) considered the effect of the initial configuration of coiled tubing on buckling, and found that this has higher impact on the axial force required to initiate helical buckling compared to the impact it has on sinusoidal buckling.

Qiu (1998) studied the contact force in drill pipe and coiled tubing. The contact force for three different cases (straight, deviated and curved wellbore) was calculated for drill pipe and coiled tubing application. The method of the Lagrange multipliers was used to define constraint (contact) forces, and no boundary conditions were imposed at the two ends of the coil. Deli et al. (1998) proposed an analytical solution for helical buckling in a horizontal wellbore using equilibrium, and a perturbation method. The effect of torque was also considered in their work. Qui et al. (1998) studied the effect of initial shape of CT string in sinusoidal and helical buckling in a constant curvature wellbore. Kuru et al. (1999) performed experimental tests to study the force transmission in horizontal and curved wellbore models, and examined experimentally the effect of internal pressure and boundary conditions. Li (1999a and 1999b) presented a formulation for buckling and dynamical behavior of rod and pipe in a wellbore: in his buckling formulation, the effect of weight was not considered. Qui (1999) studied the effect of the initial

configuration of drill pipe and coiled tubing on contact forces, by using Lagrange multipliers and energy methods. Aadnøy and Andersen (2001) presented analytical friction models based on constant curvature and catenary curve for different wellbore configurations. The torque and drag models that were presented in this paper provided analytical solutions for pickup and lowering down of drill string. Duman et al. (2001) performed experimental tests to study the effect of tool joint in the buckling of the drill pipe in a straight horizontal wellbore. Mitchell (2002) developed an analytical solution for the buckling of a pipe in a horizontal wellbore. McSpadden and Newman (2002) presented a "stiff string" model as opposed to the "soft string" model for Coiled Tubing operation. The review paper by Cunha (2003) gives an overview of the theoretical and experimental work published to date. A three-dimensional Finite Element solution was applied to the force transmission problem in coiled tubing application by Newman (2004). Terry et al. (2004) compared their model for the prediction of the surface weight indicator against field data. Mitchell (2004) studied the impact of torque and shear on buckling of drill pipe using large-displacement analysis. Mitchell (2006) studied the effect of friction on the initiation of buckling of rotating and non-rotating pipes. Sun and Lukasiewicz (2006) presented a new buckling modeling in a sucker rod pumping system.

The effect of downhole vibration in drilling operations has been studied for many years by several researchers. One of the solutions in CT intervention for extended reach application is the application of a downhole vibrating tool. The vibration in the drilling string is induced by rotational motion. Chronologically, the study of vibration in drilling caused by rotational motion precedes the application of downhole vibration in CT operations. Apostal et al. (1990) studied

the forced, damped frequency response of the bottom hole assembly (BHA) in drilling strings using the FEM. Heisig and Neubert (2000) presented an analytical criterion for critical speed in drilling application in horizontal wells, and compared their results with a finite element solution. Sola and Lund (2000) studied the effect of the downhole vibrating tool on CT operations in extended reach well. In their modeling, they used Coulomb friction for CT string and BHA in straight wellbore. Laboratory results for testing the "Friction Drag Reducer" tool showed the efficient of concept of introducing downhole vibration to CT applications.

Barakat et al. (2005 and 2007) conducted experiments to study the effect of hydraulically induced downhole vibrations in CT interventions in extended reach applications. They focused on measuring the effect of friction on the contact force distribution, and substantiated their research with experimental tests. Newman et al. (2007A) studied methods to improve microhole CT drilling operations in a research funded by US Department of Energy. Eliminating the downhole tractor or any other tools to reduce downhole friction was among the objectives of their study. They investigated the possibility of introducing surface vibration in order to reduce downhole friction between CT string and wellbore. A number of different tests were performed to measure the effect of vibration in CT input and output forces. In their report, they concluded that the surface-induced vibration mitigated downhole friction in a small scale when the axial force in the CT string exceeded the helical buckling load. In a subsequent work, Newman et al. (2007B) presented the effect of axial and rotational vibration of the CT string on the reduction of the downhole friction, based on conducted surface tests. The variation of the rotational speed can cause undesirable effects on a CT string. Newman et al. (2009) performed

experimental tests to study effect of downhole vibration on force transmission during the CT operation. They presented the field results considering the effect of downhole vibration on the maximum predicted reach for CT string. Pabon et al. (2010) used the Finite Rigid Body (FRB) modeling approach to study the effect of downhole vibration in drilling string on drilling applications, and were able to capture the transient behavior of the drill string. Tikhonov and Safronov (2011) studied the effect of torsional and drill string considering friction in the wellbore. Wicks et al. (2012) presented a one-dimensional dynamic model to study the effect of downhole axial vibration in extending the CT string reach. Tikhonov et al. (2013) presented a dynamic model for torque and drag calculation for the entire drill string. In this approach, torque, bending stiffness, contact force and friction were considered. Guo et al. (2013) presented a model to describe the behavior of CT string in extended reach wellbore using the downhole vibrating tool. The downhole vibrating tool that was modeled in this study is based on the pressure pulse wave, and the effect of pressure pulsing was considered on friction reduction and string length change.

Newman et al. (2014) performed parametric modeling to examine the influence of different parameters on increasing Coiled Tubing intervention in extended reach application. Oyedokun and Schubert (2014) studied a combination of rotating and non-rotating coiled tubing configurations in extended reach application.

Chapter 3. Coiled Tubing Services

Coiled Tubing (CT) is a very long and continuously milled pipe, which is manufactured in different sizes and lengths, and is used as a conveyance means to perform different types of well services, workover, completions and drilling operations in the oil and gas industry. The nomenclature “Coiled Tubing services” refers to the use of Coiled Tubing, surface equipment and downhole tools.

Coiled Tubing services consist of several main components such as: Coiled Tubing string, CT reel, Gooseneck, Injector head, CT power pack, CT control cabin, stripper, blowout preventer (BOP) and downhole tools. Coiled tubing services can be mobilized for both offshore and onshore operations. A Coiled Tubing equipment rig-up configuration is shown in Figure 3-1.

In onshore operations, CT reel, injector head, power pack and control cabin are mounted on trailers. The rest of the equipment is mounted on auxiliary trailers. In offshore operations, all CT equipment comes in skid-mounted frames. Skid-mounted equipment are transported by ship to offshore rigs or installations.

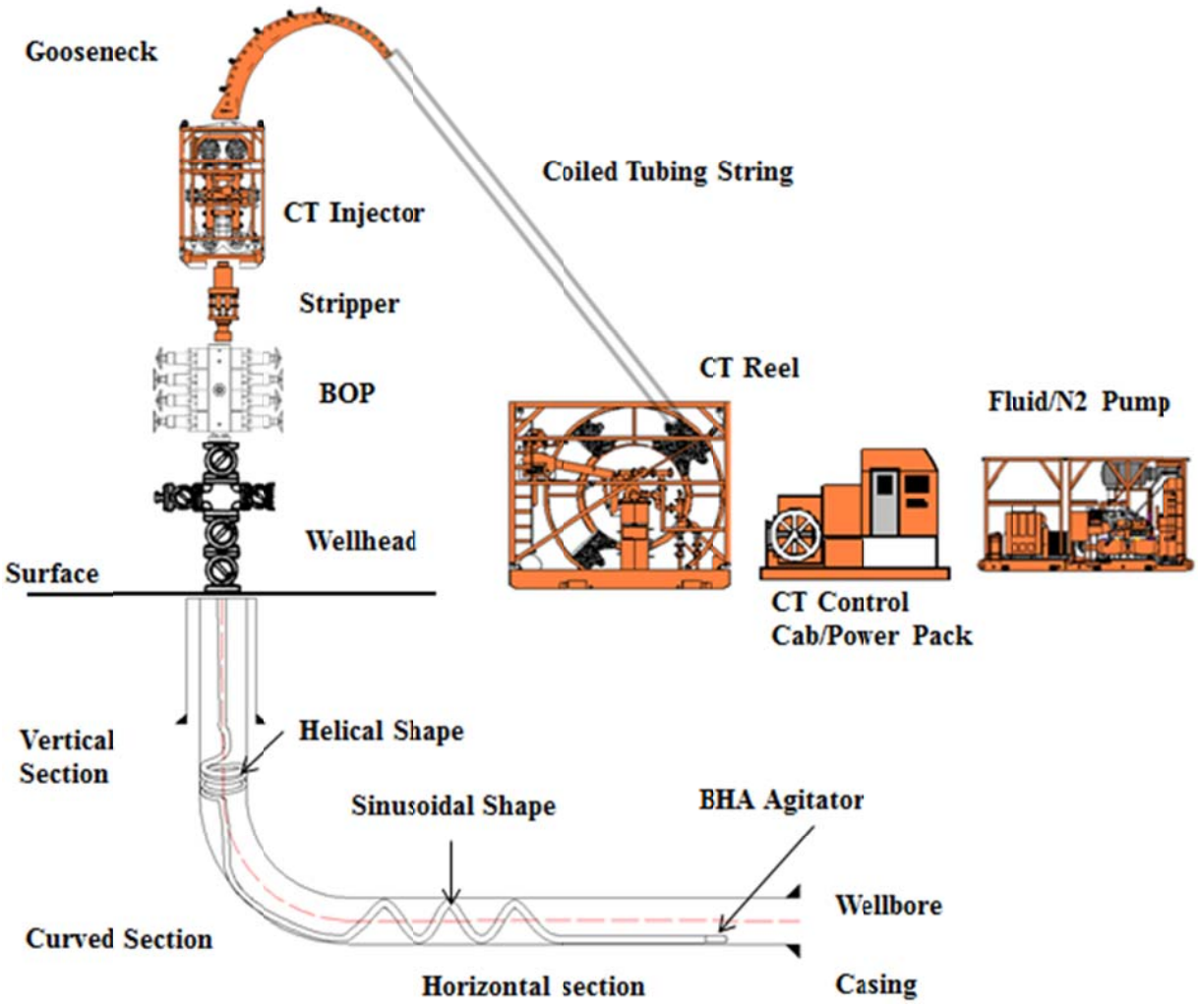

Figure 3-1: Coiled Tubing equipment rig-up configuration

Fluid pump and nitrogen pump are two extra pieces of equipment which accompany every CT operations. Either or both pumps are required for every operation, depending on the nature of the operation. Coiled Tubing services are utilized in both vertical and horizontal wellbore to provide solutions for different well services and workover problems.

The deployment of Coiled Tubing for the well interventions has a number of advantages over other options such as workover rig or drilling rig. The main advantages are listed below:

- Continuous operation in live well (producing well)
- Reduced footprint of equipment and minimized environmental impact
- Reduced number of personnel to perform job
- Faster mobilization, rig-up/rig-down of equipment and, as a result, savings in operating time
- Better well control during operation
- Faster and more efficient deployment and retrieval of CT string needed to perform required treatments

3.1. Coiled Tubing Equipment

In following sections, the main components of Coiled Tubing services are introduced.

3.1.1. Coiled Tubing String

The coiled tubing string is the main component of CT services. The CT string is a long pipe which is used to deploy in a wellbore to perform well services and workover operations. It is manufactured from metal strips with different widths, wall thicknesses and materials strength. The methods of continuously-milled tubing or butt-welded tubing section are used to shape metal strips into the desired pipe geometry. Later on, bias weld or butt weld is used to connect different strip sections to manufacture the final CT string product. A CT string comes with different outside diameter (OD): the most common diameters are 38.10 mm (1.50 in), 44.45 mm (1.75 in),

50.80 mm (2.00 in) and 60.32 mm (2.375 in). For every CT size (OD), there are several different wall thicknesses available, ranging from 2.41 mm (0.095 in) to 5.69 mm (0.224 in). The wall thickness provided for each OD varies from different manufacturers. CT strings can be designed in straight (single wall thickness) or tapered (multiple wall thicknesses) configurations.

The choice of materials and their strength are two important specifications in identifying a CT string. Low carbon steel alloys are often used. These materials are capable of withstanding the sourness of the environment (due to the presence of H_2S), corrosion and fatigue, while maintaining the high strength required for different applications. The typical yield strength of CT strings are: 482.63 MPa (70,000 psi), 551.58 MPa (80,000 psi), 620.52 MPa (90,000 psi) and 758.42 MPa (110,000 psi).

3.1.2. Coiled Tubing power pack unit

The power pack unit provides hydraulic power to different components of the CT equipment, and includes different controls to actuate hydraulic components such as pressure control valves. There are several hydraulics pumps to provide power and control for each hydraulic circuit. The main hydraulic circuits are: Injector head, Reel drive, BOP, Levelwind (travelling block) override, Priority and Auxiliary. These hydraulic pumps are driven by a diesel engine (offshore skid or trailer mounted unit). Hydraulic pumps, control valves and return tank are connected together by hydraulic hoses.

Other components in the power pack units are: hydraulic fluid, hydraulic tank, heat exchanger, hoses, filters, strainers and pressure control valves. Depending on different CT equipment manufacturers, there are several types of power pack units available, based on their

hydraulic design. Different hydraulic designs are standard open-loop, high pressure open-loop and close-loop power pack. A power pack skid unit is shown in Figure 3-2.

Figure 3-2: Power pack skid unit

3.1.3. Coiled Tubing Control Cabin

The control cabin in the CT equipment package is where the operator controls the deployment and retrieval of CT string into the wellbore by hydraulic controls. Hydraulic controls, pressure gauges, electronic sensors, data acquisition system, engine control, principal gauges and communication system are installed in the control cabin. Hydraulic controls valves enable the operator to adjust the pressure required for the Run In Hole (RIH) and Pull Out Of Hole (POOH) of the string with injector drive. The operation of CT reel drive, travelling block, open and closing of stripper (dynamic seal) and Blow Out Preventer (BOP) is done by means of designated pressure control valves in the control cabin. There are several pressure gauges the in

control panel which allow the operator to monitor air supply pressure, priority pressure, injector directional control valve pressure, injector motor pressure and reel pressure. Several electronic sensors are utilized to measure depth of the CT string (through a depth encoder), well head pressure (WHP), circulating pressure (CIRC) inside string, fluid/nitrogen pump pressure and rate. A data acquisition system collects the various CT job parameters, such as CT depth, CT speed, wellhead pressure, circulating pressure, weight of string (via a weight indicator), pump pressure and pumping rate in real-time, and relays all the information to the computer of the unit for monitoring for the duration of every job. In the engine control section of the control panel, the operator has access to engine throttle, emergency shut down button, air supply gauge and engine RPM. Primary gauges in the control panel are the weight indicator, which measures the weight of string in RIH/POOH, wellhead pressure (WHP) and circulating pressure (CIRC). During every CT job, wireless communication devices are provided to each party involved in CT operation and all directed to control cab where CT supervisor/CT engineer supervising the job. A schematic diagram of a Coiled Tubing control unit is shown in Figure 3-3.

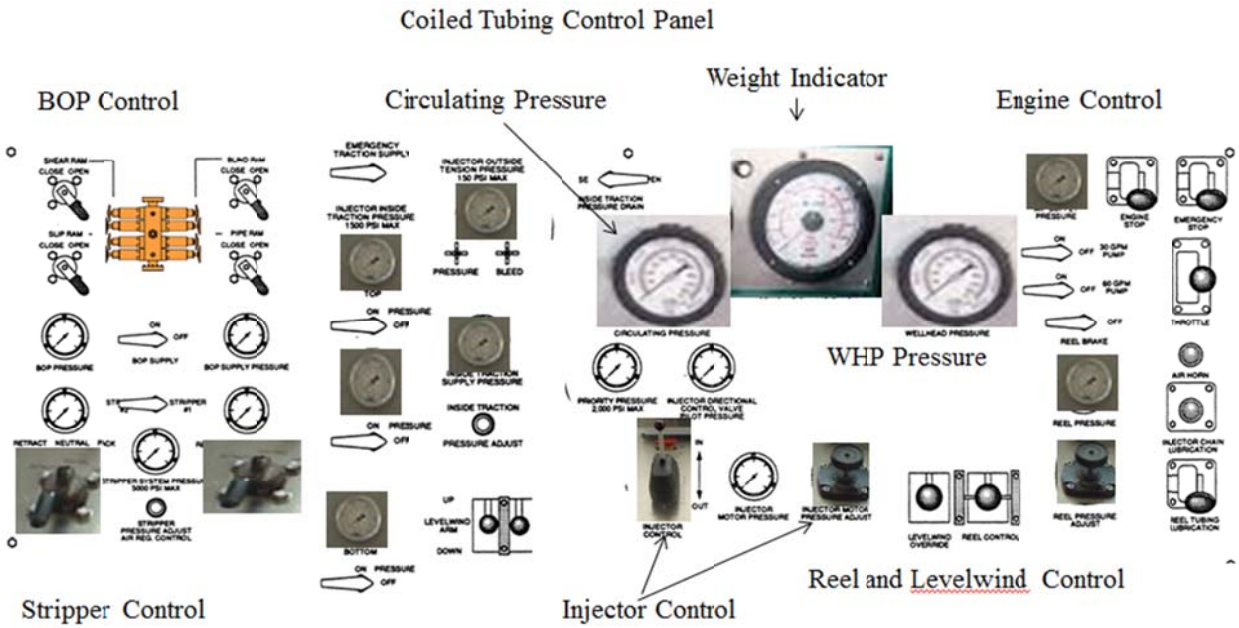

Figure 3-3: Coiled Tubing control unit

3.1.4. Coiled Tubing Reel

The main function of the CT reel is to store the CT string and protect it against damage. The CT reel comes skid-mounted for offshore operation or trailer-mounted for land operations and consists of drum (spool), level-wind assembly (travelling block), high pressure treating lines and swivel assembly, depth measurement (mechanical counter) and Reel hydraulic drive mechanism. The drum is a spool on which string is stored. We remark that the string undergoes a plastic bending deformation in order to be stored on the drum. The reel dimensions, such as core diameter, flange width and tubing stack height, dictate the length of the CT that can be stored on the drum, for each CT diameter. The level-wind assembly is a mechanism which ensures the proper arrangement of the pipe as it is been stored on the drum. The travelling block moves in synchrony with the reel and allows for the proper arrangement of the pipe in subsequent wraps.

A small hydraulic motor can override the motion of the travelling block if a correction is required for a proper spooling procedure. The high pressure manifold and swivel assembly consists of different elements of “treating irons” (i.e., high-pressure piping) and allows for pumping fluid while deploying (RIH) or retrieving (POOH) the CT, during well intervention operation. The swivel mechanism provides pumping capability while maintain the rotational motion of the drum for the duration of the job. The high pressure treatment fluid travels from the fluid/nitrogen pump to the high pressure manifold and then into the CT string through the swivel joint. The next component in the CT reel is the mechanical depth counter. The depth control box provides length of CT movement in terms of depth with respect to the surface. This is a backup system for electronic depth measuring system which is explained in Section 3.1.5 about the injector head.

Finally, the CT Reel hydraulic drive mechanism provides the motion for deployment and retrieval of string in wellbore. Direct drive and right angle drive are two configurations used in CT reel equipment. In the direct drive configuration, the hydraulic motor connects directly to the drum. In the right angle drive configuration, the hydraulic motor connects to the reel drum through chain and sprocket drive. A Coiled Tubing Reel unit is shown in Figure 3-4.

Figure 3-4: Coiled Tubing Reel unit

3.1.5. Coiled Tubing Injector Head and Gooseneck

The coiled tubing string is run in hole (RIH) and pulled out of hole (POOH) by means of the injector head. Two sets of gripper blocks, which are connected to two sets of chains, inject the pipe into or retrieve the pipe out of the wellbore. Each chain drive is driven by a separate hydraulic motor. Outside chain tensioners maintain tension in the chain and avoid loosening. The inside chain tensioner system applies force on gripper blocks to keep the CT string hanging while RIH and/or POOH. Specific sizes of gripper blocks are used for each diameter of CT string. The injector brake is located on each hydraulic motor and is controlled by a valve from the control cabin. The injector head has two different speed settings, high and low, the choice of

which is dictated by the operational conditions. Injector heads are classified by maximum pulling and slack off capability. An electronic depth control exists either as a built-in module inside the hydraulic drive motor or as a friction wheel with shaft encoder below the chains. The depth and speed recorded at instant of each time are relayed to the control cabin computer and control panel. The weight indicator load cell measures tension and compression resulting by deployment and retrieval of the string in the wellbore. Similarly to the depth encoder, the weight indicator sends all measurements to the control cabin data acquisition system for monitoring and design comparison purposes. The gooseneck (Guide Arch) is an arc-shaped structure installed on top of injector, whose function is to guide the CT string coming from the reel to the injector head in vertical position. Roller blocks on the gooseneck provide support for the string, which comes from the reel with a certain angle. Goosenecks come in different radii, ranging from 1.82 m (72 in) to 3.04m (120 in). A CT injector head and gooseneck are shown in Figure 3-5.

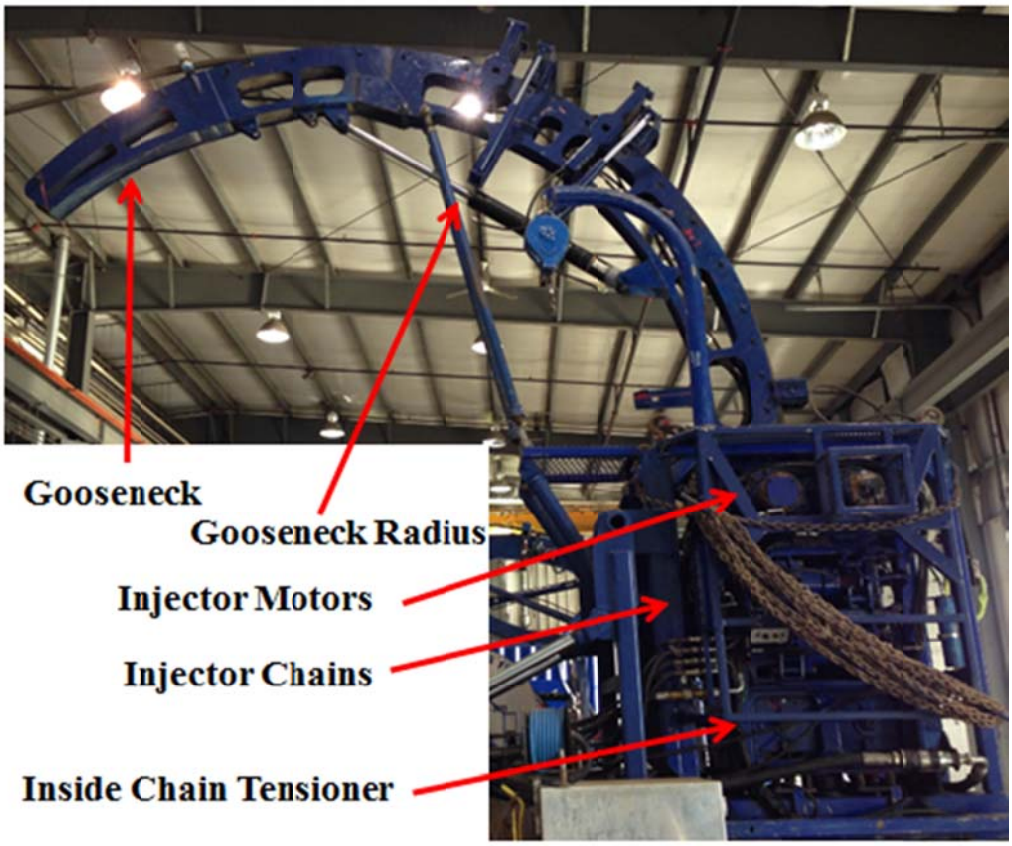

Figure 3-5: Coiled Tubing injector head and Gooseneck

3.1.6. Stripper (Stuffing Box)

One of the main applications of Coiled Tubing is in live wellbore conditions. In other words, the CT string can be deployed and retrieved while the well is in production. The element which provides such capability is called stripper (Stuffing Box). The stripper is a dynamic seal surrounded the CT string and is a part of the well control stack in a CT rig-up configuration. Hydraulic pressure is applied to a set of elastomeric rubbers. The stripper is located below the injector chains, and the hydraulic pressure on the stripper can be via the controls available in the

CT control cabin. There are a number of different Stripper designs used in CT operations: Conventional, Side-Door and Radial. A CT Stripper (Stuffing Box) is shown in Figure 3-6.

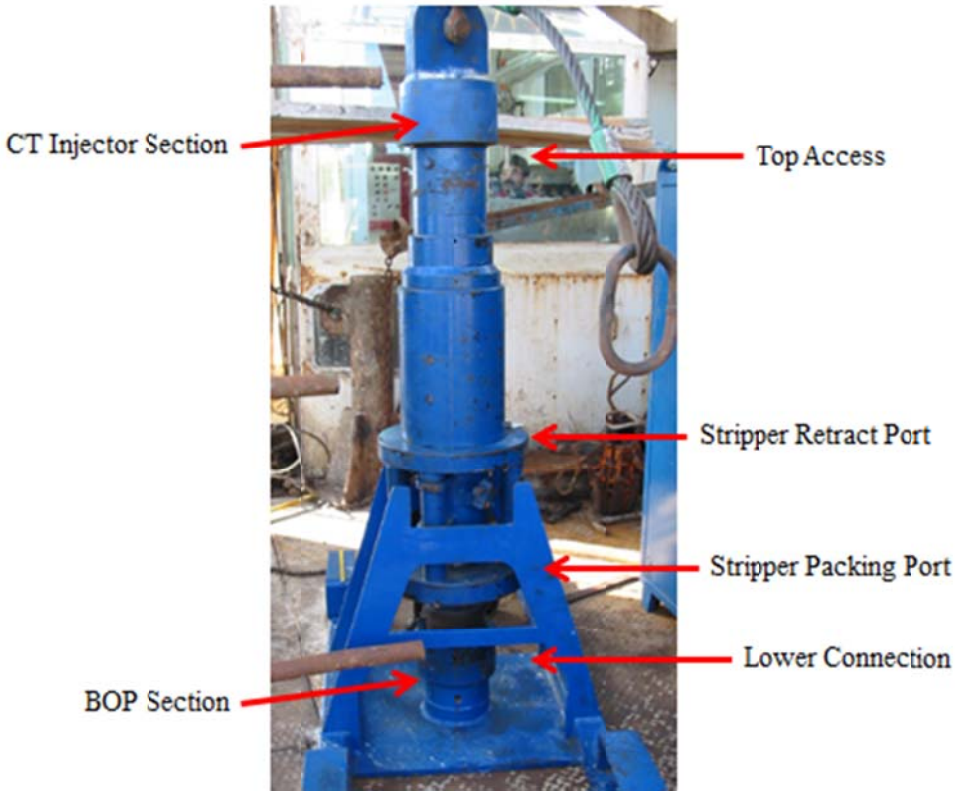

Figure 3-6: Coiled Tubing Stripper (Stuffing Box)

3.1.7. Blowout Preventer (BOP)

The Blowout Preventer (BOP) is the main well control stack element in Coiled Tubing equipment. Its main function is to control the well during well intervention operations, by containing the wellhead pressure and avoiding the release of wellbore fluid and pressure into the atmosphere. The BOP is located below the stripper and on top of the wellhead connection, and is controlled by a specific hydraulic circuit located in CT power pack. BOP controls for different

functions are located in the CT control cabin. There are four hydraulic rams on every conventional BOP: Blind, Shear, Slip and Pipe rams assembly. The blind rams seal the wellbore and do not allow the passage of fluid from the wellhead. The function of the shear rams is to cut the pipe during an emergency in well control or on a stuck-pipe situation. On both side, the shear rams contain blades designed to cut the pipe. The function of the slip rams is to hold the pipe in place and prevent the pipe from being pushed out of the well or from falling into the wellbore. Finally, the pipe rams seal the area surrounding the pipe and isolate the wellbore while the pipe is still hanging from the slip rams. There are other components in BOP such as the kill port, equalizing valves, pressure port and top/bottom connections. There are different types of BOP designs and configurations, based on operational requirements, classified as Quad BOP, Dual Combi BOP and single BOP rams. A schematic diagram of a Coiled Tubing Blowout Preventer (BOP) is shown in Figure 3-7.

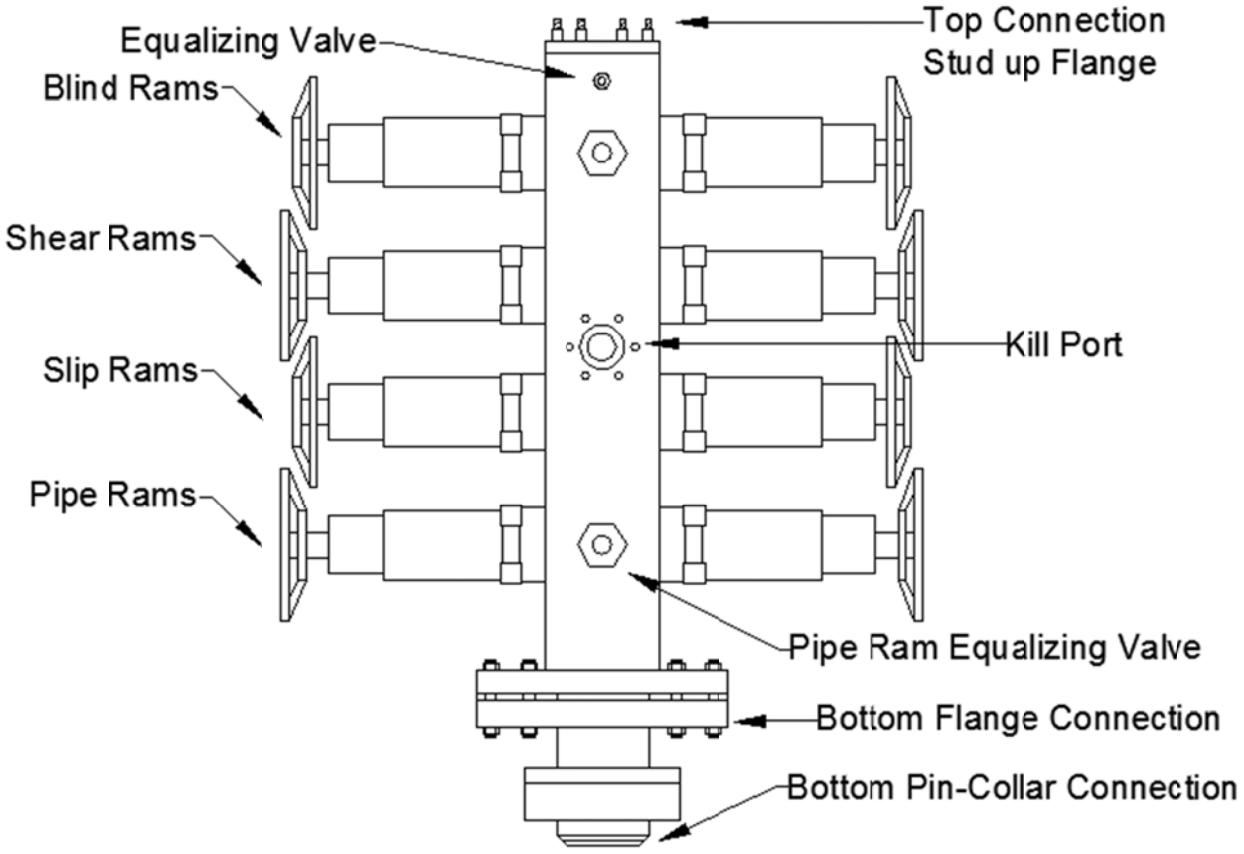

Figure 3-7: Coiled Tubing Blowout Preventer (BOP)

3.1.8. Downhole Tools

The downhole tools constitute the bottom hole assembly (BHA), which is an integral part of every Coiled Tubing operation. On very CT job, downhole tools are selected and connected to end of the CT string prior to start of the operation. The operation objectives and wellbore completions dictate which type of downhole tools is required. However, there are several components that are used on almost every operation, regardless of the nature of job. These common components, called collectively Motor Head Assembly (MHA), are the CT

connector, check valves, Disconnect and Circulating components. The first component of every downhole tool is the CT connector, which connects to the end of the string with different gripping methods such as dimple, roll-on and grapple. Once the CT connector is installed on the string, the rest of downhole tools screw in on the bottom of the connector. Double check valves prevent the influx of wellbore fluid into the string as it RIH or POOH. The next component in the Motor Head Assembly is the CT Disconnect. When the BHA gets stuck in the wellbore, the CT Disconnect is activated and the CT string is free to be retracted to the surface. The release mechanism in the CT Disconnect is either mechanically activated or pressure activated. The last component in the MHA is the circulating component, which provides extra circulating ports when high-rate pumping is required, and is activated by ball drop or pressure differential.

In addition to the MHA, there is a wide range of different downhole tools available , depending on the objectives of the operation. There are specific downhole tools for different operations such as cleanout, milling, logging, fishing, perforating, cementing, drilling, acidizing, velocity string and fracturing. A schematic diagram of a Downhole Bottom Hole Assembly (BHA) is shown in Figure 3-8.

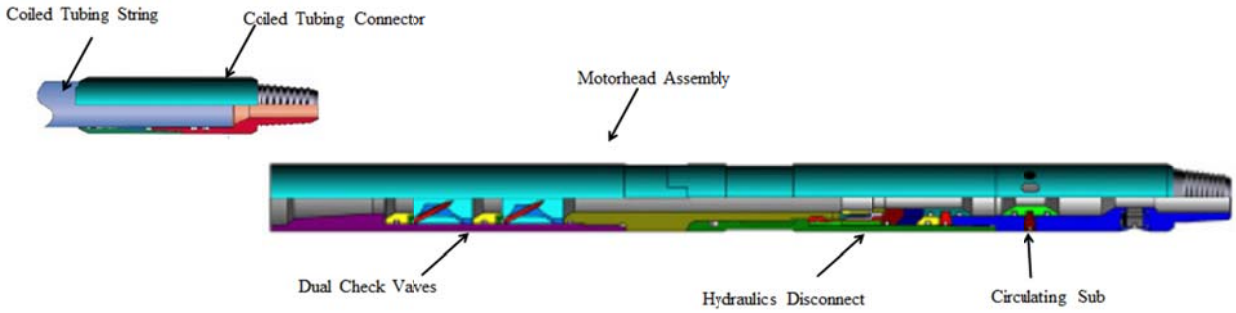

Figure 3-8: Downhole Bottom Hole Assembly (BHA) – (Bakke Oil Tools Catalog 2001)

3.2. Coiled Tubing Applications

Coiled Tubing is used in different types of well intervention operations. Based on the nature of required well intervention, a specific type of Coiled Tubing application is selected and executed. In the following, the different types of CT intervention applications are introduced.

3.2.1. Coiled Tubing Cleanout

The most common application of Coiled Tubing is fill cleanout from wellbore. The main objective of a cleanout operation is removing fills such as scales, debris, sands, wax, asphalt etc., in order to restore well production and prepare the wellbore for the next well services and workover operations.

The cleanout is achieved by pumping treatment fluid into the wellbore and circulating it out of the wellbore. In order to do so, it is necessary to add a viscous gel to the treatment fluid and to create a high annular velocity (i.e., the velocity of the fluid in the annular cross-section

between the CT and the wellbore). Another method employs a treatment fluid containing nitrogen, and its purpose is to energize the fluid and increase the annular velocity for proper cleanout.

3.2.2. Coiled Tubing Milling

One of the methods in the completion of horizontal reservoirs is fracturing services. Plug and perforation is one of the methods used with fracturing , in order to complete horizontal reservoirs. Prior to each stage of fracturing, a plug is set and the corresponding zone of interest is perforated, which exposes the reservoir to the fracturing treatment. Once fracturing is completed, it is required to remove all isolation plugs from the wellbore. At this stage, Coiled Tubing is required to perform milling. The Coiled Tubing conveys a milling tool, consisting of a number of components such as, MHA, Jars, downhole vibrating tool, motor and mill. Coiled Tubing and milling tool are used to remove the plugs and circulating debris out of the wellbore. As mentioned before, the plugs can be milled under live well condition.

3.2.3. Coiled Tubing Logging

Open-hole and cased-hole logging are methods to obtain information about a reservoir by using different suits of downhole sensors. Traditionally, Wireline provides this type of operation in vertical and deviated wellbores. One of the methods to perform logging in highly deviated and horizontal completions is the application of Coiled Tubing. The electronic line (e-line) is inserted into the CT string to provide a medium to transfer information from downhole sensors to the surface. In this way, the CT string is enabled to perform logging in open-hole and

cased-hole completions. The logging head downhole tool connected to the end of CT provides a platform for different Wireline sensors to be attached to CT string. One of the most common applications of Coiled Tubing logging is production logging. By deploying a CT equipped with an e-line, the production data are captured and relayed real-time to the surface . The deployment of a downhole camera is among other application of CT strings with e-line.

3.2.4. Coiled Tubing Matrix Stimulation (Acidizing)

The decline in production rate, compared to the potential production capacity of a reservoir, is one of the important challenges in the life cycle of an oil/gas well. The production decline could be the result of near-wellbore restrictions (perforations) or formation damage. Considering reservoir parameters and well testing data, one of the means to tackle this problem is matrix stimulation, which includes washing perforations and the injection of acid treatment fluids into the formation in order to reduce the damage in reservoir or to establish new paths in the reservoir to recover the expected production rate. CT is used to pump different acid treatment fluids while moving the CT string across the targeted intervals.

3.2.5. Coiled Tubing Drilling

One of the methods to increase production in low pressure matured reservoirs is to drill a new lateral “leg” in the main wellbore. A low reservoir pressure requires an underbalanced intervention while the well is producing. Underbalanced drilling avoids reservoir damage due to overbalanced conventional drilling solutions. From an economic perspective, hydrocarbon production during drilling makes the operation more cost-effective. A Coiled Tubing drilling

package is capable of drilling a new lateral leg in underbalanced conditions. A specialized drilling BHA is conveyed with a CT string to drill the lateral leg connected to the main wellbore. The application of nitrified drilling fluid ensures a low bottom hole pressure, yet maintaining enough medium to carry the cuttings resulting from drilling to the surface. A specially designed drilling tower is required in CT drilling. The drilling well control stacks ensure a safe and controlled condition while the well is producing.

3.2.6. Coiled Tubing Fracturing

One of the completion methods in shallow vertical wellbores is Coiled Tubing fracturing. A straddle packer type is used as the downhole tool in this application. The straddle packer isolates the zone of interest at each stage. High-pressure treatment fluid mixed with sands (slurry) is pumped down through the CT string into an isolated zone to fracture each reservoir interval. The use of CT fracturing services provides multiple fracturing in a single wellbore. High-pressure nitrogen-based fluid or CO_2-based fracturing fluid are injected through CT string to perform fracturing. Employing this method of intervention reduces the completion time and cost, in addition to improving post-treatment cleanup and production.

3.2.7. Coiled Tubing Cementing

Coiled Tubing is used to perform cement squeeze and cement plug placement jobs, which are required in cases of well abandonment, casing repair, zonal isolation and water gas shutoff. Cement squeeze is a process which cement is forced into the formation by means of the application of pressure through perforations in the wellbore. Cement plug placement is a process

which a designed volume of cement is spotted in the wellbore to isolate sections of the reservoir. CT cementing is the application of pumping cement slurry through the CT string in order to squeeze cement or place a cement plug in a wellbore. The use of Coiled Tubing cementing provides precise placement and a lower contamination of the cement slurry due to a lower exposure to the wellbore fluid.

3.2.8. Coiled Tubing Fishing

The retrieving of a lost BHA, parted string, dropped object or bridge plug is a procedure called “fishing”, for which a CT string can be used (CT fishing), even in a live well. There is a wide variety of downhole tools available, depending on the nature of the fishing operation. The stiffness of CT and the possibility to deploy the CT in a horizontal wellbore are among the advantages of such intervention. In attempting to latch on the fish, pumping through the CT string can activate a fishing BHA. The Circulation of different types of fluid in the CT string assists the retrieval process. For the case of a stuck fish, the CT can safely exercise designed pull or slack off in order to free up the fish.

3.2.9. Coiled Tubing Nitrogen Kick off

When hydrostatic pressure of column of wellbore fluid exceeds reservoir pressure, well production is ceased. Nitrogen kick off job through CT string is required to recover well production. Pumping nitrogen though CT string at designed depth reduces wellbore fluid density; therefore, wellbore hydrostatic pressure is reduced. By reducing downhole pressure reservoir stars producing. Nitrogen pump unit delivers nitrogen gas through CT string.

3.2.10. Application of Coiled Tubing Equipped with Optical Fibers

CT strings equipped with optical fibers are among the latest developments in Coiled Tubing services. An optical-fiber-equipped string is injected inside the CT string and functions as a data delivery medium for downhole information. The major advantage of an optical fibers CT string compared to an e-line CT string is its ability to capture the thermal logging of the entire wellbore during operation for a wide variety of applications, including gas well production logging, matrix stimulation, leak detection, Fracture monitoring, Water injection etc. Moreover, the diameter of an optical fiber is smaller than that of an e-line, which allows for pumping different treatment fluids with high “pumping rate” (i.e., flow) while receiving real-time downhole information .

3.3. Job Design Considerations for Coiled Tubing Services

Prior to every Coiled Tubing job, it is required to examine and verify the feasibility of the intervention operation. This includes tubing force modeling (TFM), fatigue analysis of the CT string and the evaluation of the pressure limits of the CT string during the operation. In tubing force modeling, the design engineer determines whether or not the selected CT string can reach to the desired depth to perform required operation.

As a CT string deploys into a wellbore, a drag force between CT string and wellbore develops. Therefore, the more the CT string runs through the wellbore, the more drag forces occur, and therefore the more axial force is required to continue running the CT string. Once the axial force increases to a certain threshold, CT string turns into a sinusoidal buckling configuration. This

threshold value of the axial force is called sinusoidal load or $F_{\text{Sinusoidal}}$. As the CT continues running in hole (RIH), the axial compressive force increases and, at certain load, the CT string turns into a helical buckling configuration. This load is called helical buckling load or $F_{Helical}$. When the CT string turns into the helical buckling mode, the drag force starts to increase dramatically. Indeed, the contact force between CT string and wellbore increases as a result of the increasing axial compressive force. When the force at the surface (slack-off weight) cannot be transferred to the downhole end, the CT string stops and no further progression is possible. This situation is called “lock-up”.

In order to calculate the lock-up depth, it is necessary to use wellbore data which can be summarized as: wellbore trajectory (Measured Depth, Inclination Angle and Azimuth Angle), wellbore casing configurations and wellbore completions components. Friction in the wellbore plays an important role in developing contact forces between CT string and wellbore. There are several methods to reduce the effect of friction and the contact forces. One of such methods is the application of a downhole vibration, which shall be explained in Section 3.4. When it has been evaluated that the CT string can reach to the desired depth, two more criteria need to be checked from an operation perspective: the fatigue life of the CT string and the operating pressure envelope of string. These two design considerations are not the subject of this study.

3.4. Downhole Vibrating Tool

One of the main challenges of Coiled Tubing intervention in a long horizontal wellbore is reaching to the target depth. As mentioned above, as the CT string progresses in the horizontal

section, the friction between CT string and wellbore increases, resulting in sinusoidal buckling first and then in helical buckling. One of the means to eliminate or attenuate this problem is the application of a downhole vibrating tool, which is a part of the downhole bottom hole Assembly (BHA). The function of the downhole vibrating tool is to create a longitudinal vibration mode in the CT string, which helps reducing the contact forces between wellbore and CT string. Therefore, the CT string can progress further in wellbore and maximize its reach.

One brand of downhole tool vibrating tool is called “Agitator” and it is manufactured by National Oil Varco (NOV, Houston, TX, USA). The Agitator tool consists of power section, valve and bearing. The power section is basically a downhole motor which drives the valve section. The valve and Bearing sections in turn generate pressure pulses which cause an axial vibration motion in the CT string. The hydraulic energy of the pumped fluid is converted into mechanical vibration by the Agitator. The downhole vibration generated by the Agitator reduces the wellbore friction drag and allows for more force to be transferred from surface to downhole. A schematic diagram of a downhole vibrating tool (Agitator) is shown in Figure 3-9.

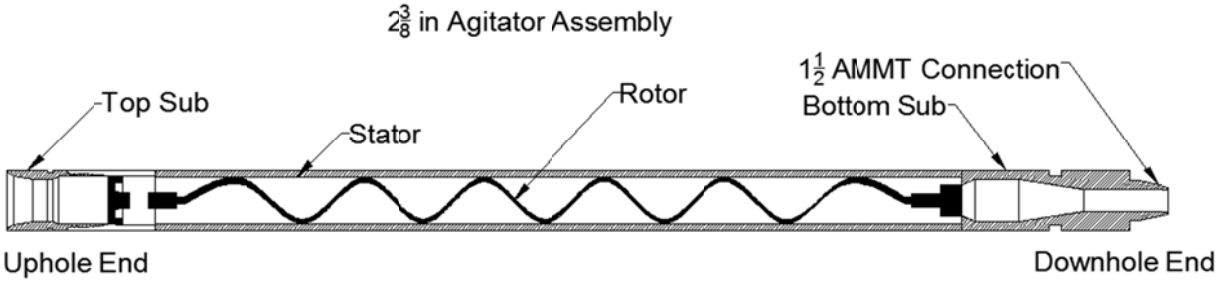

Figure 3-9: Downhole vibrating tool (Agitator)

Chapter 4. Theoretical Background

In this chapter we report the existing theoretical relationships used in modeling a buckled tubing inside a wellbore as follows:

- Force-pitch relationships
- Sinusoidal and helical buckling load criteria
- Contact force for sinusoidally/helically buckled string in a horizontal wellbore
- Axial force transmission relationships for a horizontal wellbore
- Soft string model
- Lock-up condition

Lubinski et al. (1962) presented the effect of helical buckling in a packer-tubing system for several different configurations. The pitch-force relationship for helically buckled tubing was developed based on energy methods. As shown in Figure 4-1, a string is hung in a vertical wellbore without fluid in the casing, and a compressive Force (F) is applied to the downhole end of the tubing. When this force is large enough (above the helical buckling force) the downhole section of the string below the neutral point turns into the shape of a helix. The "neutral point" in the string is the cross-section which is neither in tension nor in compression (Lubinski on et al. 1962). The cross-sections above the neutral point (neutral cross-section) are all in tension, and the ones below are all in compression.

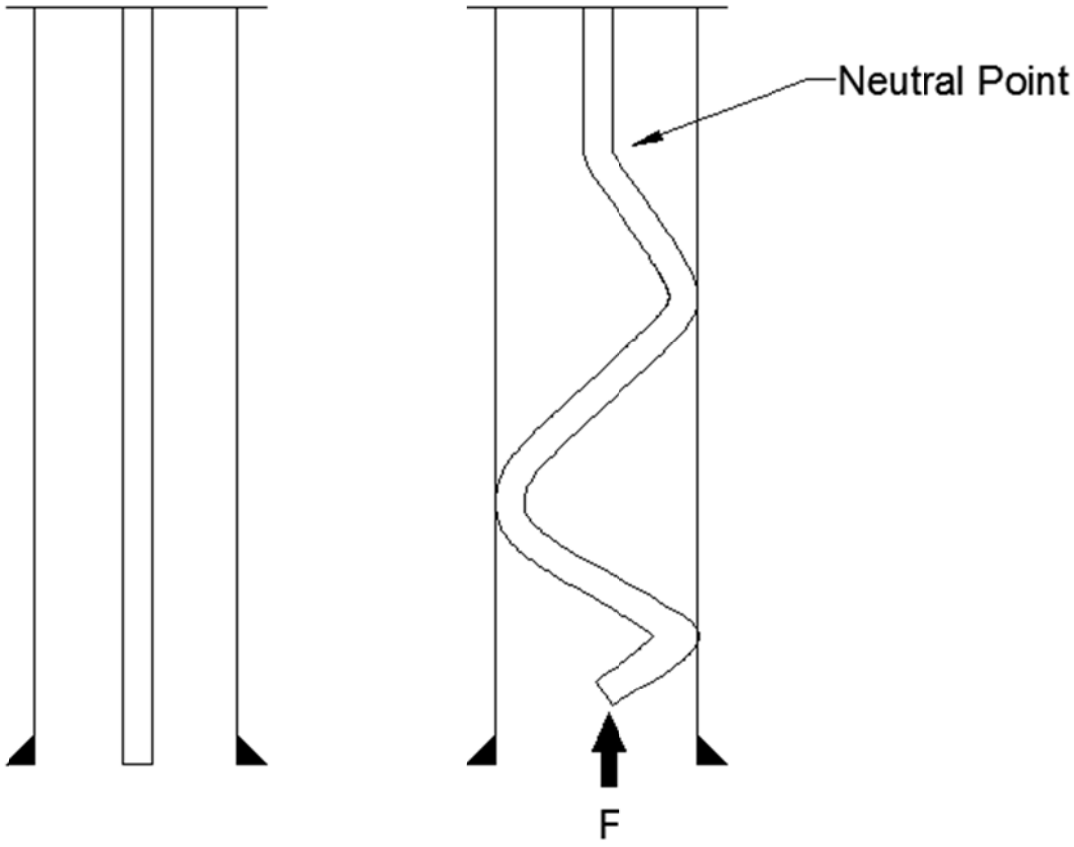

Figure 4-1:Buckling of string in wellbore

The location of the neutral point is given by the expression

$$n = \frac{F}{w}, \tag{4.1}$$

Where n is distance from the end of tubing to the neutral point in m (in), F is the compressive force (positive) in N (lb) and w is weight of pipe per unit length in air in N/m (lb/in).

The relationship between pitch (Figure 4-2) and compressive force (for helical buckling section) is described by Equation (**2.1**) (see Appendix A for details). Solving Equation (**2.1**) for pitch yields:

$$p = \pi\sqrt{\frac{8EI}{F}}, \tag{4.2}$$

where p is the pitch of the helical portion of the string in m (in), E is the Young's modulus in Pa (or psi; for steel, E = 206.8 MPa or 30E6 psi), I is moment of inertia in m^4 (in^4) and F is the compressive force (positive) along the axis of the helix in N (lb). The pitch-force relationship is developed by the application of energy methods. The strain energy for axial compression is given by (see Appendix A- Equation A-3)

$$U_c = \frac{1}{2}\frac{L}{EA_s}F_a^{\,2}, \tag{4.3}$$

where F_a is the compressive force along the axis of the string, L is the length of the string not subjected to compressive force (initial length) and A_s is cross-sectional area of the tubing wall.

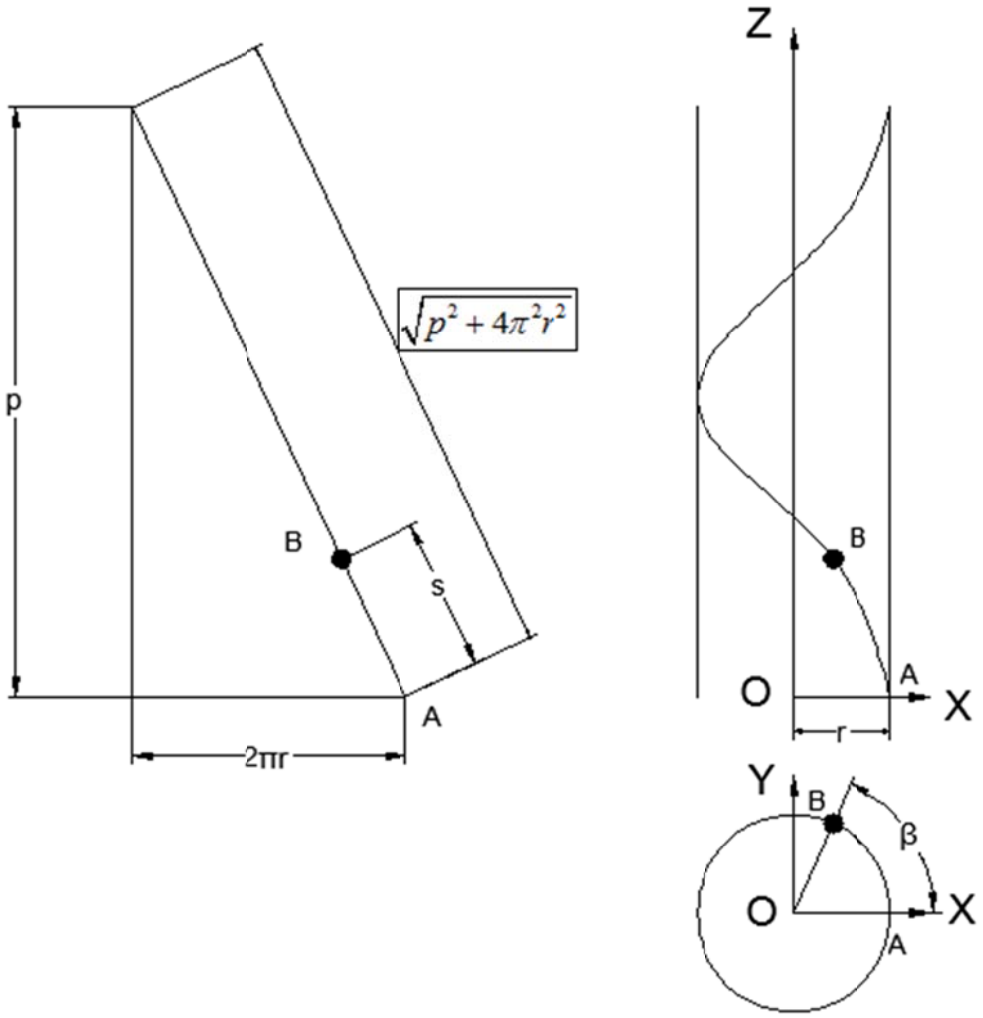

Figure 4-2:Helix geometry and pitch of buckled string

The strain energy for bending is defined as

$$U_{bending} = \frac{1}{2} LEI\, C^2, \tag{4.4}$$

where C is the curvature of the helix, i.e.,

$$C = \frac{4\pi^2 r}{p^2 + 4\pi^2 r^2}. \tag{4.5}$$

The potential energy (for the force *F*) is:

$$U_f = FL_h, \tag{4.6}$$

where

$$L_h = \frac{L_c p}{\sqrt{p^2 + 4\pi^2 r^2}}, \tag{4.7}$$

is the length of the helix measured along its axis, and

$$L_c = L\left[1 - \frac{F \sin\theta}{EA_s}\right], \tag{4.8}$$

is the length of the string undergoing compression .

The total energy for this system is defined as the sum of the strain energies of axial compression and bending and the potential force, which yields

$$U = -\frac{F^2 p^2 L}{2A_s E(p^2 + 4\pi^2 r^2)} + \frac{8\pi^4 r^2 EIL}{(p^2 + 4\pi^2 r^2)^2} + \frac{FpL}{\sqrt{p^2 + 4\pi^2 r^2}}. \tag{4.9}$$

By minimizing the potential energy with respect to the pitch, i.e., by imposing $dU/dp = 0$, the pitch-force relationship is driven as (see Appendix A for details)

$$F = \frac{8\pi^2 EI}{p^2}. \tag{4.10}$$

Paslay and Bogy (1964) studied the stability of a rod in a constrained cylindrical geometry using energy methods and assuming that the rod maintains constant contact with the cylindrical constraint (wellbore), and the tubing curvature does not change. The loads on the rod consist of its weight (gravitational forces), axial force and moment at both ends (Figure 4-3). In order to find the stability criteria, the total potential energy of this system must be minimized. The total potential energy can be written as

$$V = U + \Omega, \tag{4.11}$$

where U is elastic strain energy and Ω is the work of the external forces.

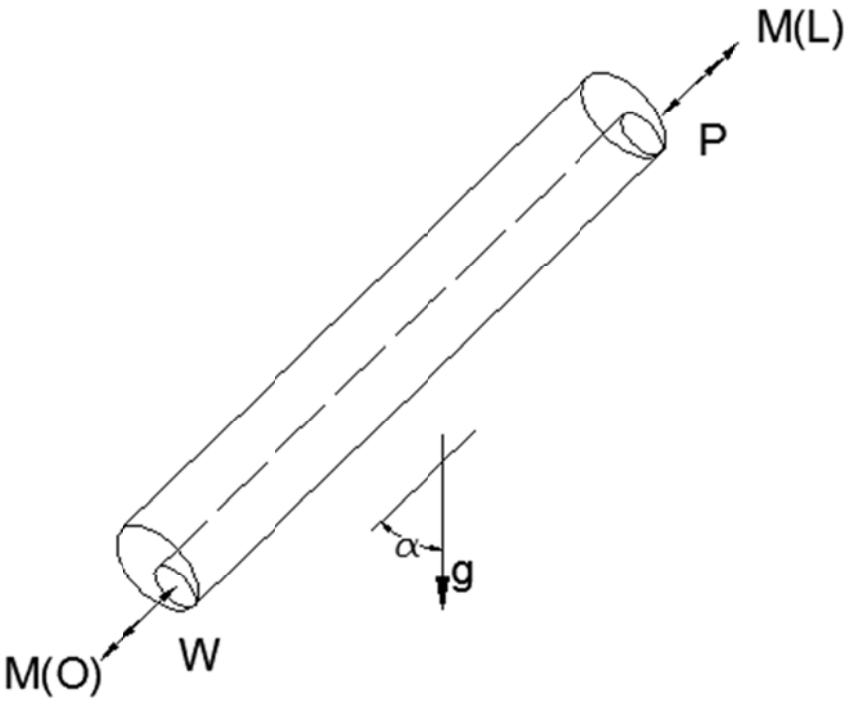

Figure 4-3: Configuration of a string in a wellbore

The change in total potential energy (ΔV) for this system is:

$$\Delta V = \delta U + \delta\Omega + \frac{1}{2!}\delta^2 U + \frac{1}{2!}\delta^2\Omega + \frac{1}{3!}\delta^3 U + \frac{1}{3!}\delta^3\Omega + \ldots . \tag{4.12}$$

Two conditions are required to minimize the total potential energy for this system, i.e.,

$$\delta U + \delta\Omega = 0 \tag{4.13}$$

which imposes an extremum on the energy, and

$$\delta^2 U + \delta^2 \Omega > 0 \tag{4.14}$$

which means that the extremum is actually a minimum. Developing the expression for the horizontal case ($\theta = 90^\circ$) and assuming that the rod is at contact with the casing (wellbore) at all times, imposing that $\delta^2 V = 0$ yields

$$P_{cr_{(n)}} = (1-\upsilon)\bar{E}I\frac{\pi^2}{L^2}\left(n^2 + \frac{1}{n^2}\frac{L^4 \rho A g}{\pi^4 E I r}\right), \tag{4.15}$$

where $P_{cr_{(n)}}$ is critical load, υ is the Poisson's ratio,

$$\bar{E} = \frac{2G(1-\upsilon)}{(1-2\upsilon)} \tag{4.16}$$

is the elastic modulus in uniaxial strain (as opposed to the Young's modulus *E*, which is the elastic modulus in uniaxial stress), L is length of rod, r is the clearance between rod and casing, ρgA is the weight per unit length of rod and n is the order of the buckling mode.

By assuming $k = \rho gA/r$ (elastic foundation constant), Equation (4.15) reduces to the solution of a finite beam on an elastic foundation. By substituting the expression of the modulus $\bar{E}$, the critical force becomes

$$F_{crit} = \frac{(1-\upsilon)^2}{(1+\upsilon)(1-2\upsilon)} EI\frac{\pi^2}{L^2}\left(n^2 + \frac{L^4 \rho A g}{n^2 \pi^4 E I r}\right). \tag{4.17}$$

Replacing ρAg with w and imposing $\upsilon = 0.3$ yields a multiplicative coefficient of 0.942, which can be approximated by 1, and F_{crit} becomes

$$F_{crit} = EI\left[\frac{n\pi}{L}\right]^2 + \frac{w}{r}\left[\frac{L}{n\pi}\right]^2 \quad . \tag{4.18}$$

The first buckling mode ($n=1$) is found by minimizing F_{crit}, i.e. (Dawson and Paslay,1984),

$$\frac{\partial F_{crit}}{\partial n} = 0 \quad , \tag{4.19}$$

which yields

$$n^2 = \sqrt{\frac{L^4 w}{\pi^4 EIr}} \quad , \tag{4.20}$$

and

$$F_{crit} = 2\sqrt{\frac{EIw}{r}} \quad , \tag{4.21}$$

where F_{crit} is the required compressive force for the rod to transition to the sinusoidal configuration in horizontal wellbore (see Appendix B for details).

As the axial load continues increasing above the sinusoidal buckling load, the rod turns into a helical configuration once the axial load reaches the helical buckling load. The helical buckling load can be derived by minimizing the energy function with respect to $m = L/p$ (number of full waves in buckled pipe). The strain bending energy U_b, the external work W_e and the potential energy V are

$$U_b = \frac{8\pi^4 EILr^2}{(L/m)^4}\ , \tag{4.22}$$

$$W_e = \frac{2FL\pi^2 r^2}{(L/m)^2}\ , \tag{4.23}$$

$$V = wLr\ , \tag{4.24}$$

respectively. The total energy U is the set to zero (Chen et al., 1989),

$$U = W_e - U_b - V = 0. \tag{4.25}$$

Solving the above equation with respect to F yields the helical buckling force

$$F^* = 4EI\left(\frac{m\pi}{L}\right)^2 + \frac{w}{2r}\left(\frac{L}{m\pi}\right)^2. \tag{4.26}$$

By minimizing the helical buckling force (F^*) with respect to number m of full waves in the buckled rod, i.e.,

$$\frac{\partial F^*}{\partial m} = 0\ , \tag{4.27}$$

the helical buckling load is derived as (see Appendix C for details)

$$F^* = \left(2\sqrt{2}\right)\sqrt{\frac{EIw}{r}}\ . \tag{4.28}$$

When the axial compressive force exceeds the sinusoidal buckling load, the string transitions into a sinusoidal configuration. Therefore, a new contact force is developed. In order

to calculate the sinusoidal contact force in the wellbore, energy methods are again applied to a half sine-wave buckling deflection in a horizontal wellbore (Figure 4-4). The wall contact force under conditions of sinusoidal buckling wall contact force was evaluated by Wu (1995) as

$$N_{Sin} = \frac{rF^2}{8EI}. \tag{4.29}$$

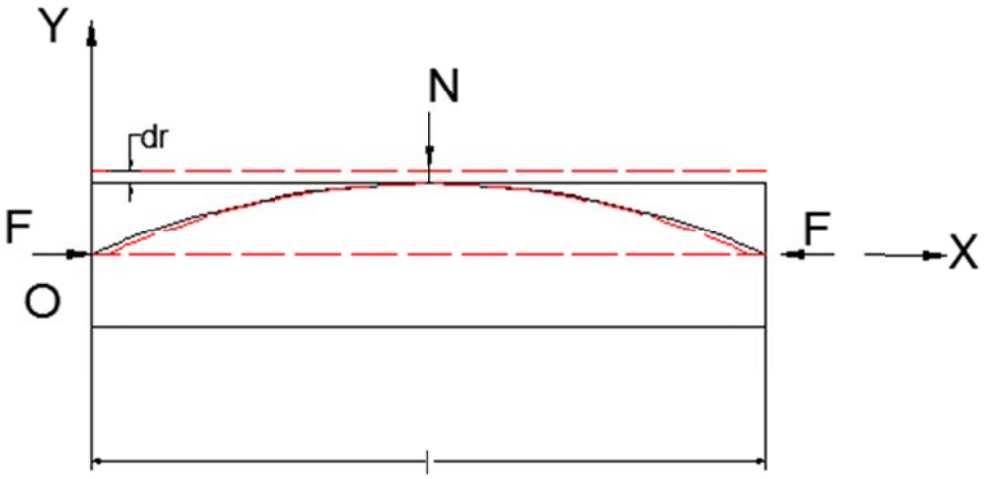

Figure 4-4: Sinusoidal buckled string in horizontal wellbore

As the compressive axial load continues to increase and becomes greater than the helical buckling load, the string transitions into a helical configuration, and a new contact force develops. As for the case of the contact force in sinusoidal buckling, the contact force in helical buckling in a horizontal wellbore as been calculated using energy methods as (Wu, 1995)

$$N_{Hel} = \frac{rF^2}{4EI}. \tag{4.30}$$

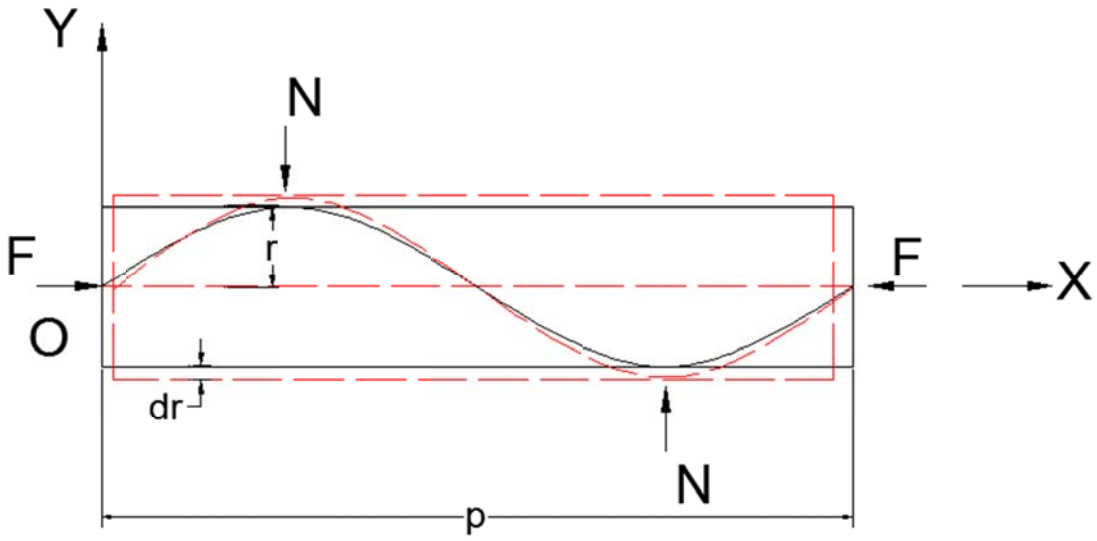

Figure 4-5: Helical buckled string in horizontal wellbore

In and inclined wellbore, the friction force for an unbuckled pipe is (Wu and Juvkam, 1993c)

$$F_f = \mu w_e \sin\theta \ , \tag{4.31}$$

where θ is the angle of wellbore with respect to the vertical, μ is the friction coefficient and w_e is effective weight of the pipe per unit length. The axial force for an unbuckled pipe in an inclined wellbore has been derived as (Wu, 1995)

$$F(x) = F_0 + \left(\mu W_e \sin\theta - W_e \cos\theta\right) x, \tag{4.32}$$

where F_0 is the axial load at the downhole end ($x = 0$) and x is measured along the wellbore axis from the downhole end.

For a horizontal wellbore ($\theta = 90^\circ$, Figure 4-6) this expression reduces to (Wu, 1995)

$$F(x) = F_0 + (\mu W_e)\, x\,. \tag{4.33}$$

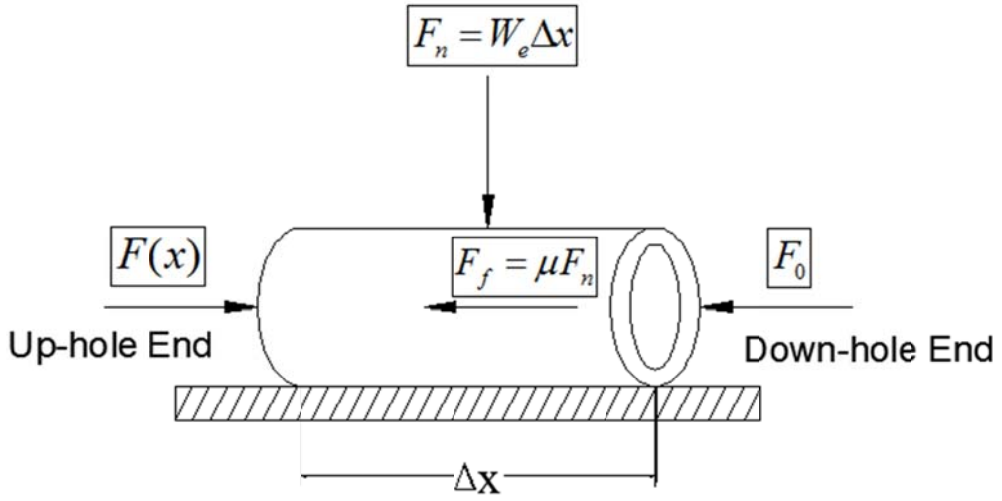

Figure 4-6: Force balanced in horizontal wellbore

When the tubing turns to the sinusoidal or helical buckling shape (i.e., the axial force exceeds the sinusoidal or helical buckling load), an extra drag force is introduced to the system as a result of contact forces. The axial force for such case is no longer linear. The overall contact force, consisting of drag (due to sinusoidal/helical contact) and weight of the pipe is (Wu and Juvkam, 1993c)

$$w_t = w_n + w_e \sin\theta, \tag{4.34}$$

where w_t is the overall contact force per unit length between pipe and wellbore wall, w_n is the contact force per unit lenght resulting from the helical buckling of the pipe and w_e is the effective weight of pipe per unit length in wellbore.

The force balance for an element of pipe undergoing sinusoidal/helical buckling in an inclined wellbore can be expressed by (Wu and Juvkam, 1993c)

$$\Delta F = \mu w_t \Delta x - w_e \cos\theta \Delta x = \left(\left(w_e \sin\theta + w_n \right) \mu - w_e \cos\theta \right) \Delta x \ , \tag{4.35}$$

from which

$$\frac{dF}{dx} = \mu \left(w_e \sin\theta + w_n \right) - w_e \cos\theta \ , \tag{4.36}$$

and using the expression of w_n,

$$\frac{dF}{dx} = \mu \left(w_e \sin\theta + \frac{rF^2}{4EI} \right) - w_e \cos\theta \, . \tag{4.37}$$

The axial force corresponding to sinusoidal and helical shapes can be derived by applying expressions of the contact forces for sinusoidal/helical buckling, which have been already calculated in Equations (**4.29**) and (**4.30**).

The axial force distribution for sinusoidally buckled pipe in a horizontal wellbore is (Wu, 1995)

$$F(x)=\sqrt{\frac{8EIW_e}{r}}\tan\left\{\mu x\sqrt{\frac{rW_e}{8EI}}+\arctan\left(F_0\sqrt{\frac{r}{8EIW_e}}\right)\right\}, \tag{4.38}$$

and for a helically buckled pipe in a horizontal wellbore is (Wu, 1995)

$$F(x)=\sqrt{\frac{4EIW_e}{r}}\tan\left\{\mu x\sqrt{\frac{rW_e}{4EI}}+\arctan\left(F_0\sqrt{\frac{r}{4EIW_e}}\right)\right\}. \tag{4.39}$$

To find the axial compressive load for a CT string inside a curved wellbore described by the curvilinear abscissa s, the soft string model (Bhalla, 1994) is used to describe axial load distribution as

$$dF=w\,ds\cos\theta\pm\mu\sqrt{\left(d\gamma\sin\theta F\right)^2+(Fd\theta+w\,ds\sin\theta)^2}\ , \tag{4.40}$$

where dF is the incremental change in axial force (no buckling), w is weight per unit length of the pipe, θ is inclination angle of the wellbore with respect to the vertical, and $d\gamma$ is the incremental change in azimuth angle of the wellbore survey (i.e., the curve that the wellbore describes in space), and ds is the increment in curvilinear abscissa along the wellbore survey. Positive sign applies to the pull-out-of-hole (POOH) condition and the negative sign applies to the slack-off case (or run-in-the-hole, RIH).

When the axial compressive force exceeds the helical buckling load, the axial load distribution will change and the contact force due to helical buckling must be accounted for. The incremental change in axial force for a helically buckled string is given by (Bhalla, 1994)

$$dF=w\,ds\cos\theta\pm\mu\left(\sqrt{\left(d\gamma\sin\theta F\right)^2+(Fd\theta+w\,ds\sin\theta)^2}+\frac{rF^2}{4EI}\right). \tag{4.41}$$

In this thesis, the wellbore survey lies on a plane, i.e., there is no change in azimuth angle, and therefore, we shall use Equation (4.41) with $d\gamma/ds = 0$. Moreover, the curved segment of the wellbore survey will be assumed to have a constant radius of curvature R, i.e., to be an arc of circumference, for which

$$\frac{d\theta}{ds} = \frac{1}{R}. \tag{4.42}$$

In order to show the effect of downhole vibration on the CT string, first it is required to calculate the axial compressive force in the CT string for the provided wellbore survey. The wellbore is divided into three segments: vertical, curved (heel) and horizontal. The axial force distribution relationships for the unbuckled section corresponding to vertical, curved and horizontal sections are given by

$$\frac{dF}{ds} = -w\ , \tag{4.43}$$

$$\frac{dF}{ds} = (-1)\, w\cos\left(\frac{s}{R}\right) + \mu\frac{F}{R} + \mu\, w\sin\left(\frac{s}{R}\right)\ , \tag{4.44}$$

$$\frac{dF}{ds} = \mu w\,, \tag{4.45}$$

respectively.

The axial forces increase as the CT string is deployed into the wellbore. When the axial forces reach the helical buckling load limit, the CT string turns to helical buckling shape and

axial load distribution changes for each section of wellbore due to the additional drag forces caused by the contact with the wellbore.

The criteria for helical buckling load criteria for the vertical section is (Wu and Juvkam, 1995a)

$$F_{Helical\_Veritical} = 5.55\left(EIw^2\right)^{1/3}, \tag{4.46}$$

for the curved section (with radius of curvature R) is (Qui et al.,1998)

$$F_{Helical\_Curved} = \frac{8EI}{rR} + \left(1 + \sqrt{\frac{1 + w\sin\theta rR^2}{2EI}}\right), \tag{4.47}$$

and for the horizontal section is (Chen et al.,1998)

$$F_{Helical\_Horizontal} = \left(2\sqrt{2}\right)\sqrt{\frac{EIw}{r}}. \tag{4.48}$$

When the axial compressive force exceeds the helical buckling load on each section, new load distribution relationship are required due to the extra contact forces resulting from the helical buckling. For a helically buckled string, the axial compressive load distribution in the vertical segment is (Mitchell, 1986b)

$$\frac{dF}{ds} = -w + \frac{\mu rF^2}{4EI}, \tag{4.49}$$

for the curved segment is (Bhalla, 1994)

$$\frac{dF}{ds} = (-1)\, w\cos\left(\frac{s}{R}\right) + \mu\frac{F}{R} + \mu\, w\sin\left(\frac{s}{R}\right) + \frac{\mu rF^2}{4EI}, \tag{4.50}$$

and for the horizontal segment is (Wu and Juvkam, 1993c)

$$\frac{dF}{ds} = \mu w + \frac{\mu r F^2}{4EI}. \tag{4.51}$$

One of the most important criteria to be verified on every job is whether or not the CT string can reach the desired depth to perform the operation. When the compressive axial force in the CT string exceeds the helical buckling load, the string turns to the helical shape and extra contact forces are generated. This extra drag reduces the force transmitted from the uphold end (surface) to downhole end (bottom hole) significantly. As the compressive axial force increases, less and less force is transmitted downhole. There is a critical point at which, no matter how much force is applied to the uphole end (surface), no force is transferred to the downhole end (bottom hole). This situation is called “lock-up”. Numerically, if the force transferred to the downhole section is less than 1% of the force applied uphole, the pipe reaches the lock-up condition,

$$\frac{\Delta F_{out}}{\Delta F_{in}} < 0.01, \tag{4.52}$$

and can no further proceed. This concept is depicted in Figure 4-7.

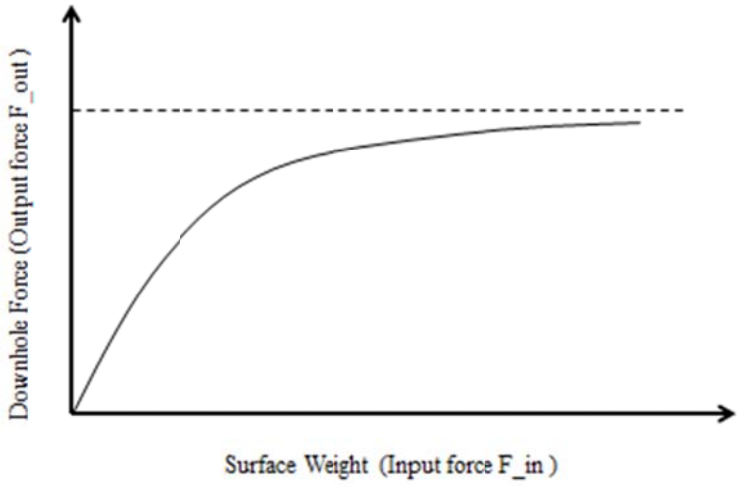

Figure 4-7: Lock-up condition graph

Furthermore, the coiled tubing may yield plastically due to the bending stress caused by the helical buckling in the wellbore (He and Kyllingstad, 1995). The maximum compressive stress in the string is given a contribution due to the axial force and a contribution due to the helical buckling, i.e.,

$$\sigma_{\max} = \frac{F}{A_s} + \frac{F(d_o/4)}{I} r \ , \tag{4.53}$$

from which the plastic yielding axial force is

$$F_y = \frac{\sigma_y}{\left(\frac{1}{A_s} + d_o \frac{r}{4I}\right)}, \tag{4.54}$$

where d_o is the outer diameter of the CT string, A_s is net cross-section of the CT string, and σ_y is the yield stress. However, normally, lock-up occurs much earlier than plastic yield.

Chapter 5. Modeling

This chapter presents the core result of this thesis: the proposed method of multiple friction factors and its application to the modeling of a full wellbore. The modeling focuses on the prediction of the improvement in force transfer and in the extension of the reach.

5.1. Modeling vs Published Experimental Data

Wu and Juvkam-Wold (1993c) validated their model of axial load distribution versus small-scale experimental data. In their experiment, they simulated the drill string by means of a brass bar with an outside diameter of 2.4 mm (0.095 in), and the wellbore by means of a plastic pipe with an inside diameter of 25.7 mm (1.012 in). The dimensions of the brass bar and plastic pipe were selected to reproduce, in a smaller scale, the geometry of the drill string and wellbore encountered in real field operations. A hand-driven screw was used to apply an axial load from the right side to the brass bar inside the plastic pipe. The applied load increased to the point where brass bar turned to the helically buckled configuration. Two load cells were attached to both sides of the brass bar in order to measure the applied axial load.

Different loads were applied via the hand-driven screw and Force In (uphole-end) and Force Out (downhole-end) were measured. The recorded data was fitted to the helically buckled model. Figure 5-1 shows the experimental data obtained by Wu and Juvkam-Wold (1993c). For a straight shape in a horizontal wellbore, the axial force starts to increase in order to buckle the pipe while input and output forces are being measured. The applied axial load is increased and, as a result, the configuration of the rod changes from straight to sinusoidal and later on to helical.

In Figure 5-2, the axial force distributions for all 3 configurations (straight, sinusoidal and helical) are shown against the experimental data. The green line represents the axial load transferred before the buckling of pipe, according to Equation (**4.32**). The red curve represents the axial load transferred when the pipe attains the sinusoidally buckled configuration, according to Equation (**4.38**). The black curve represents the axial load transferred when the pipe turns to the helically buckled configuration, according to Equation (**4.39**).

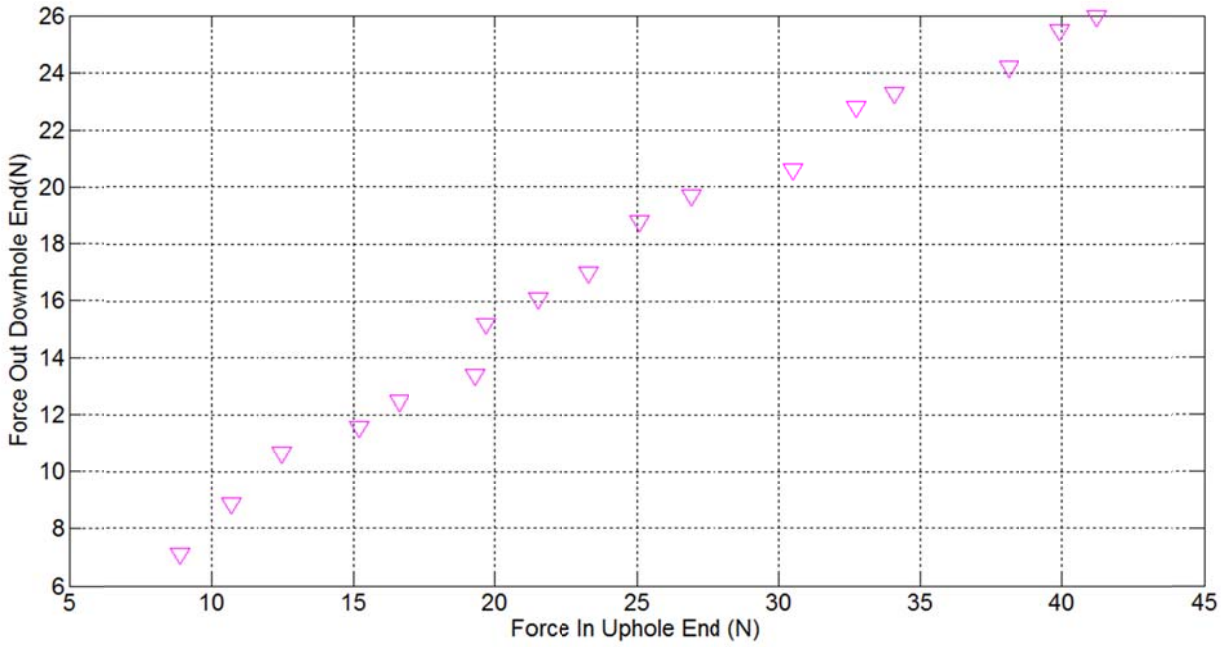

Figure 5-1: Experimental data extracted from Wu and Juvkam-Wold (1993c)

Originally, the equations for the straight and sinusoidal configurations were not used by Wu and Juvkam-Wold (1993c) and have been added in this work. In fact, Wu and Juvkam-Wold (1993c) did not present the experimental data corresponding to the straight and sinusoildally buckled sections. However, their theoretical model aimed at describing the axial load transferred

for the helically buckled section (black curve, described by Equation (**4.39**) is in close agreement with the experimental data. A deviation between the black curve (load transfer model for helically buckled section) and the experimental data is observed for high value of axial loading. This could be caused by the fact that their model considered an infinitely long string, i.e., neglected the boundary conditions.

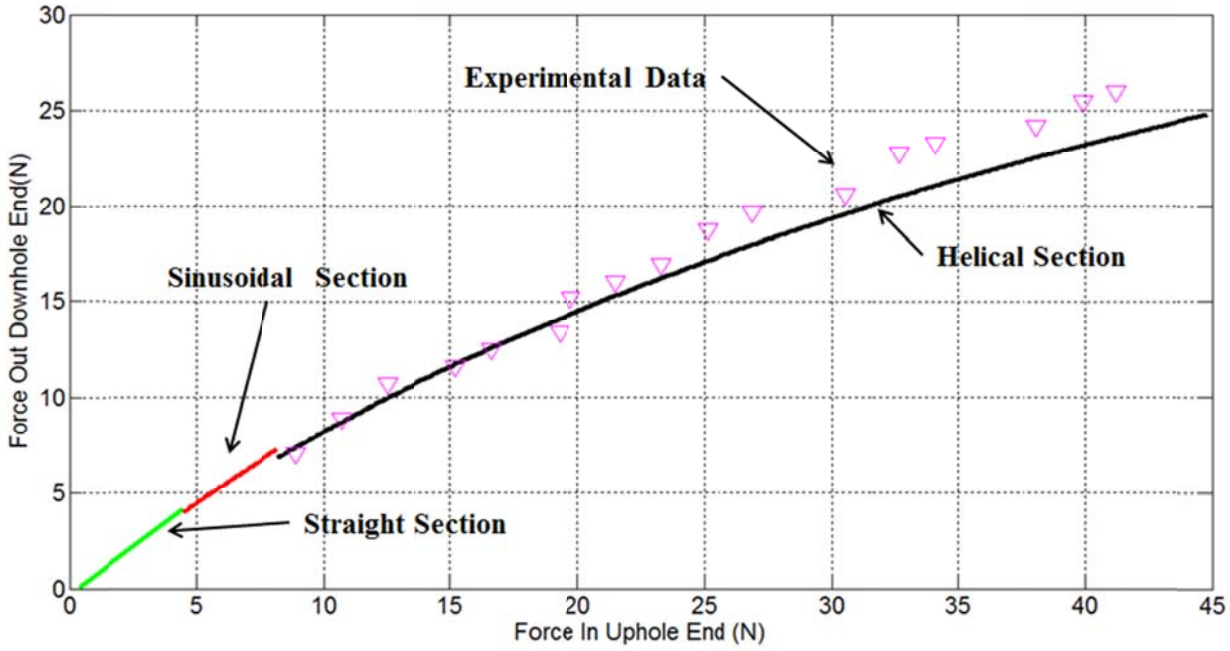

Figure 5-2: axial load distribution theoretical vs. experimental based on Wu-Juvkam test

Newman et al. (2007, A, 2007, B and 2009) conducted surface tests to investigate the effect of vibration and rotation on the reduction of friction. Several different tests were performed in straight and curved tubes, which simulated wellbores with the same geometries. In this thesis, the experimental data corresponding to the straight tube is used. A 170 m (558 ft)

long, 73mm (2 7/8 in) corrosion-resistant alloy (CRA) tubing was used as a wellbore and a CRA tubing with a 25.4 mm (1 in) outer diameter was used to model Coiled Tubing. The friction factor between casing and tubing was 0.2. The wellbore (straight tube) was fixed in place with cement blocks at several locations along the length of string. An axial force piston and a load cell were connected to one end of string to apply and measure, respectively, the "Force-In". Another load cell was connected at the opposite end of the string in the simulated wellbore, in order to measure the "Force-Out", which represented the value of force transferred downhole. Electric vibrators were used to apply vibration on the string next to the axial load piston, with a frequency of 40 Hz and an amplitude of 3114 N (700 lb). The experimental data for the force transfer, with and without axial vibration, for a straight wellbore are shown in Figure 5-3.

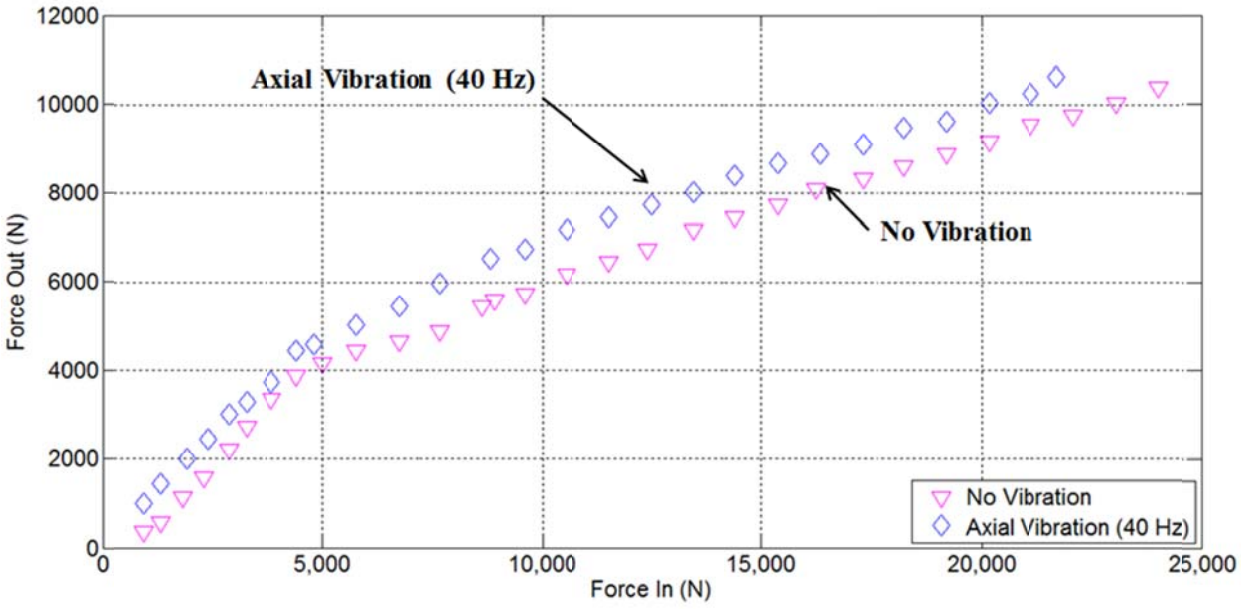

Figure 5-3: Experimental data extracted from Newman et al. (2007A, 2007B, 2009)

In this thesis, three different axial load distribution models are used to match the experimental data for the non-vibrating case. Figure 5-4 shows the axial load predicted by the models for the straight section (Equation (4.32)), sinusoidal section (Equation (4.38)) and helical section (Equation (4.39)), against the experimental data by Newmann et al. (2007A, 2007B, 2009). The closet match against the experimental data is obtained with a friction factor of 0.23, applied to all three sections (straight, sinusoidal and helical). There is a good match between theory and experimental data for the non-vibrating case.

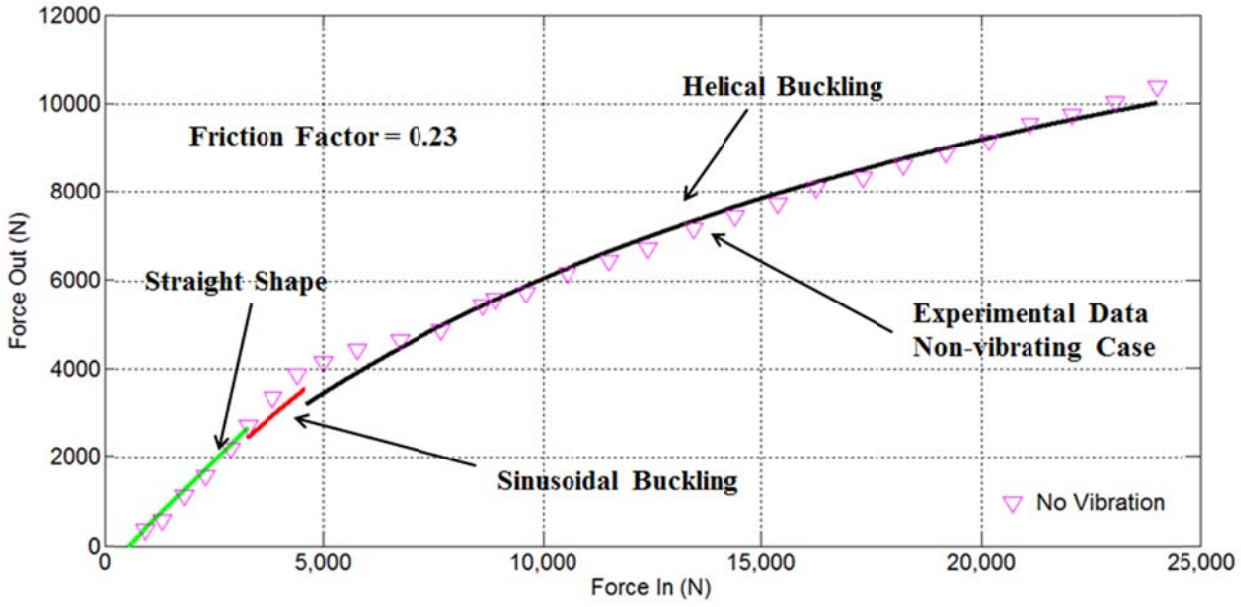

Figure 5-4: Axial loading vs Experimental data for non-vibrating case

The load distribution predicted by the models for the straight (Equation (4.32)), sinusoidal (Equation (4.38)) and helical section (Equation (4.39)) are compared the against experimental data for the vibrating case in Figure 5-5. In this case, the best match has been

obtained with a friction factor of 0.19, for all three segments. However, for the vibrating case, it is evident that the use of a single friction factor provides a poor match between model and experimental data, particularly for low values of the Force In.

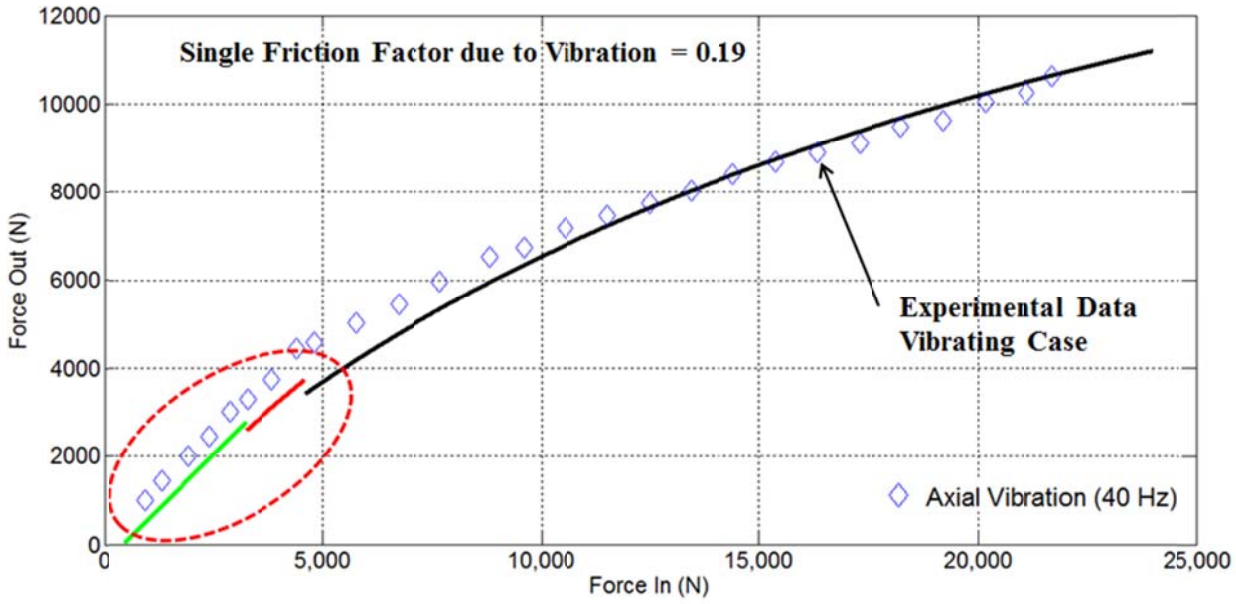

Figure 5-5: Axial loading vs Experimental data for vibrating case – single friction factor

In order to achieve a better match with the experimental data for the vibrating case, we propose to use three different friction factors (apparent friction factors) for straight (Equation (4.32)), sinusoidal (Equation (4.38)) and helical section (Equation (4.39)). In this approach, the effect of the axial vibration on the string is hypothesized to reduce the friction factor between string and wellbore. We shall show that the concept of apparent friction factor enables us to capture the effect of vibration on the reduction of friction in the wellbore and, consequently, captures the improvement in load transfer compared to the non-vibrating case.

The apparent friction factors used to match the model against the experimental data are

$\mu_{\_apparent\_straight=}0.05$ $\mu_{\_apparent\_sinusoidal=}0.09$ $\mu_{\_apparent\_helical=}0.185$

Figure 5-6 shows that the application of the three apparent friction factors does indeed provide a better match between model and experiments in the straight and sinusoidal sections for the vibrating case.

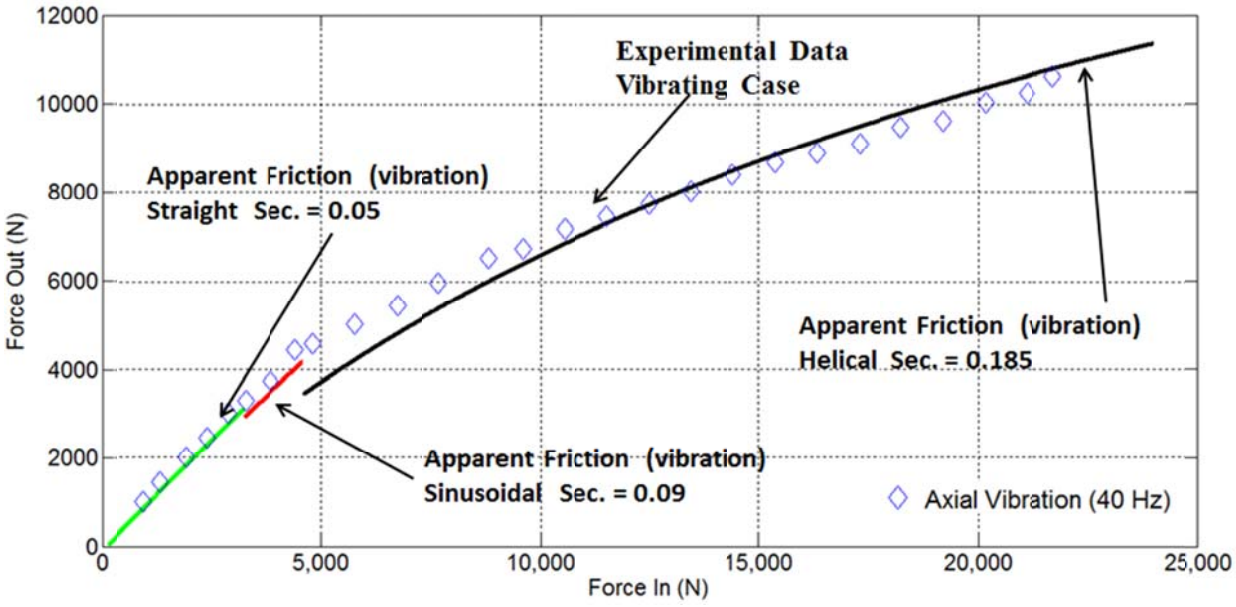

Figure 5-6: Axial loading vs Experimental data for vibrating case – multiple friction factors

Now, we propose to apply the evaluated apparent friction factors for the three segments (straight, sinusoidal and helical) to account for the effect of the application of a downhole vibrating tool in CT intervention. As shown by the experiments performed by Newmann et al. (2007A, 2007B, 2009), axial vibration increases load transfer and therefore enables to push the CT string farther in the wellbore. Figure 5-7 shows how the proposed model captures this

behavior. Indeed, a higher load transfer is achieved in the vibrating case compared to the non-vibrating case.

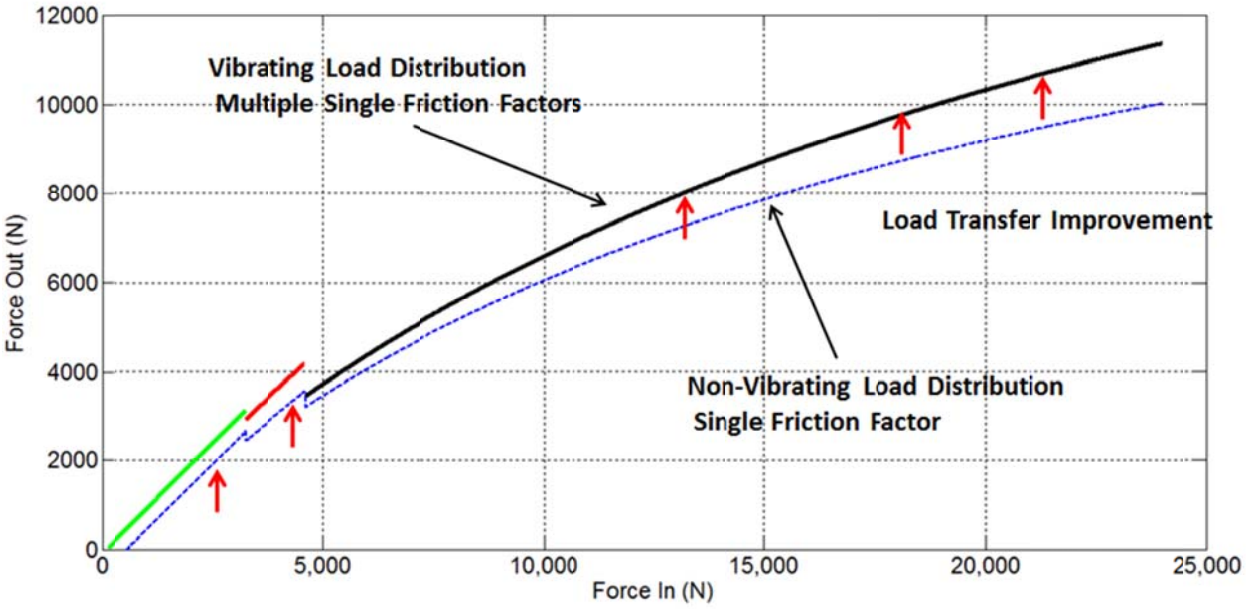

Figure 5-7: Axial Loading Models for Vibrating and Non-Vibrating Cases

5.2. Full Wellbore Modeling

Downhole vibration causes a reduction in wellbore drag and, as a result, an improvement in the depth that can be reached. The question is now: how much friction reduction is the downhole vibration tool required to provide in order to obtain a certain improvement in transferred force? Or, equivalently, in extension of the reach? This can be answered by the use of the multiple apparent friction factors. We should mention that a more accurate selection of the

friction factor would be possible if more experimental data, with different sizes of Coiled Tubing and wellbore, were available.

To perform the modeling, it is necessary to know the wellbore survey (trajectory), i.e., the path of the well from surface to the final depth. The wellbore survey is defined by coordinate system such as: measured depth, inclination angle and azimuth angle. The measured depth (MD) is the length measured along the path of the wellbore, in meters (we shall use the notation "mMD", meaning meters of measured depth; see Figure 5-8, the inclination angle is measured from the vertical axis and expressed in degrees, and the azimuth angle is measured with respect to the magnetic North Pole and expressed in degrees (Figure 5-9).

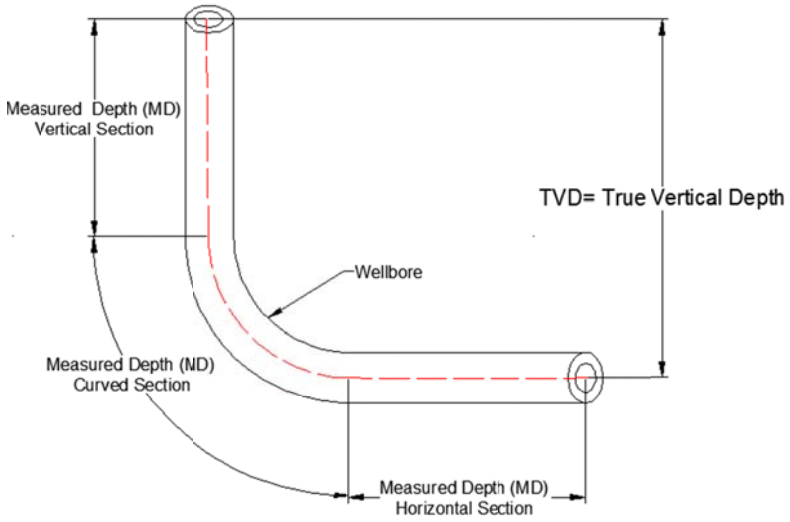

Figure 5-8: Measured depth in wellbore

Our sample wellbore (Figure 5-9) starts from surface at 0 mMD and extends to 5600 mMD. The wellbore inclination increases from 0 deg in the vertical section to 90 deg at the end of the curved section (heel section) and remains constant at 90 deg all the way through the

horizontal section. For simplicity, we assume a zero azimuth angle for this wellbore, so that its axis is entirely contained in a vertical plane (Figure 5-10). Therefore all the effects of the change in azimuth angle on the axial compressive load distribution (Equations (**4.40**) and (**4.41**)) are not considered in this study. Moreover, the radius of curvature of the curved (heel) section is assumed to be constant, so that its axis is a quarter of circumference (Figure 5-10).

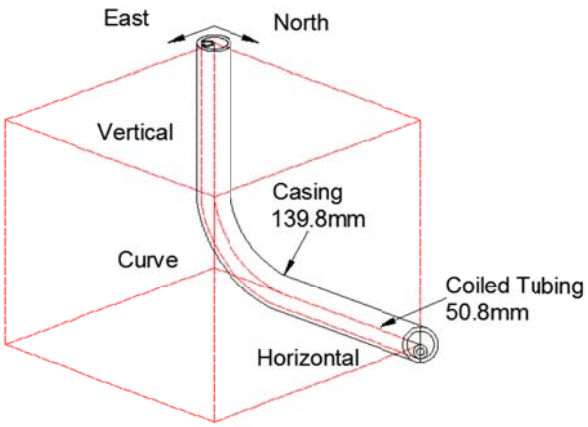

Figure 5-9: Wellbore survey in 3D

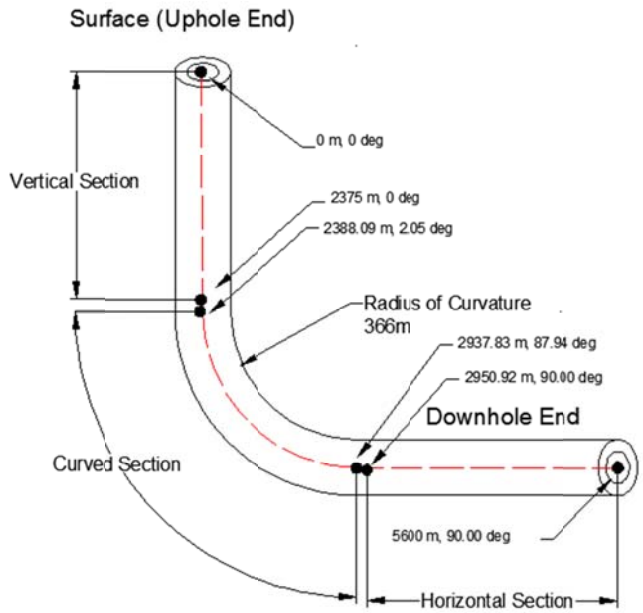

Figure 5-10: Wellbore survey in 2D

The casing (Figure 5-11) of the wellbore has a 139.70 mm (5.5 in) outside diameter, a 121.36 mm (4.77 in) inside diameter, and a 29.76 kg/m (20.00 lbm/ft) weight per unit length. The CT string has a 50.8 mm (2 in) outside diameter, a 44 mm (1.732 in) inside diameter, resulting in a 3.4 mm (0.134 in) wall thickness, a 3.98 kg/m (2.68 lbm/ft) weight per unit length, and a length of 5600 m (183723 ft), and it is made of a QT-900 grade alloy.

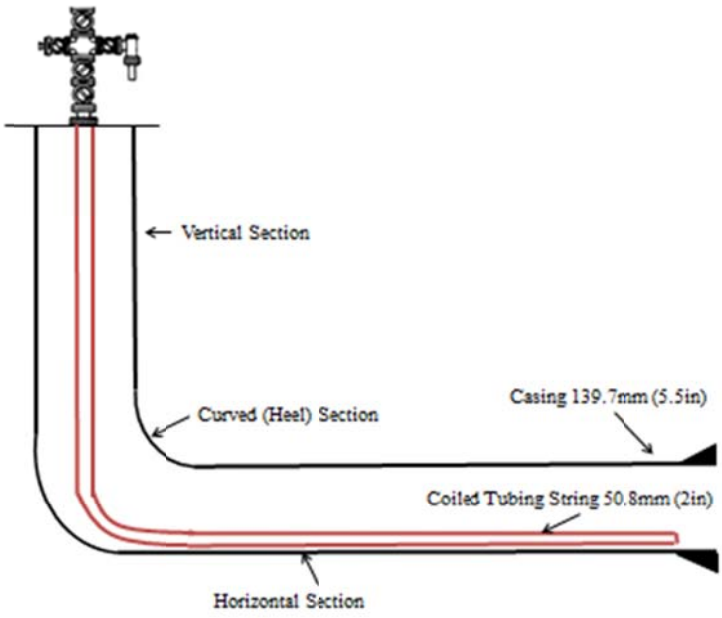

Figure 5-11: Wellbore Completions

In order to model a CT intervention job, we must evaluate whether or not the selected CT string can reach to the desired depth and establish the maximum depth achievable. Assuming a wellbore as described above, these feasibility requirements are addressed by calculating:

- the axial load distribution for the entire wellbore;
- the helical buckling load for the vertical, curved and horizontal sections of wellbore;
- the slack off weight, in order to establish the lock-up condition at a given depth.

A Matlab program was developed to calculate the axial compressive force for the Run In Hole (RIH) case (i.e., the deployment of the CT string). In this program, the axial force calculation is started from bottom hole (end of the CT string) and progresses toward the surface.

The wellbore is divided into the three sections of Figure 5-10. The axial forces for the vertical, curved and horizontal sections are calculated through Equations (4.43), (4.44) and (4.45), respectively, and compared to helical buckling loads of Equations (4.46), (4.47) and (4.48), respectively. Figure 5-12 shows the helical buckling loads for the three sections. If the CT string buckles helically, then the new axial force distributions for vertical, curved and horizontal sections are evaluated by means of Equations (4.49), (4.50) and (4.51), respectively, which account for the effect of the contact force caused by helical buckling.

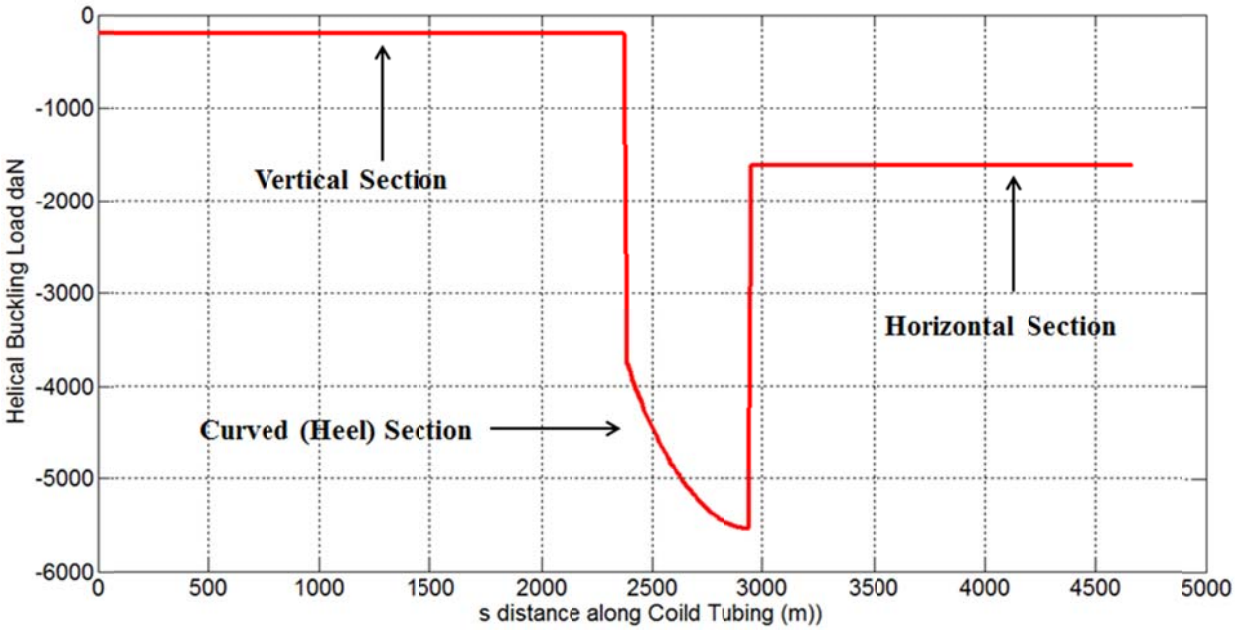

Figure 5-12: Helical Buckling Load in wellbore

From a numerical point of view, when the downhole force (F_{Out}) is less than 1% of the slack off weight (also called surface weight, F_{In}), the CT encounters lock-up and cannot reach to

the desired depth. Another Matlab program was developed to calculate the amount of force transferred downhole as a result of the slack off weight applied at the surface. The program stops once the lock-up condition is achieved.

At first, the CT string was imagined to be run to the end of the vertical section and the corresponding slack off weight calculation is shown in Figure 5-13. The lock-up condition was achieved after 127 iterations.

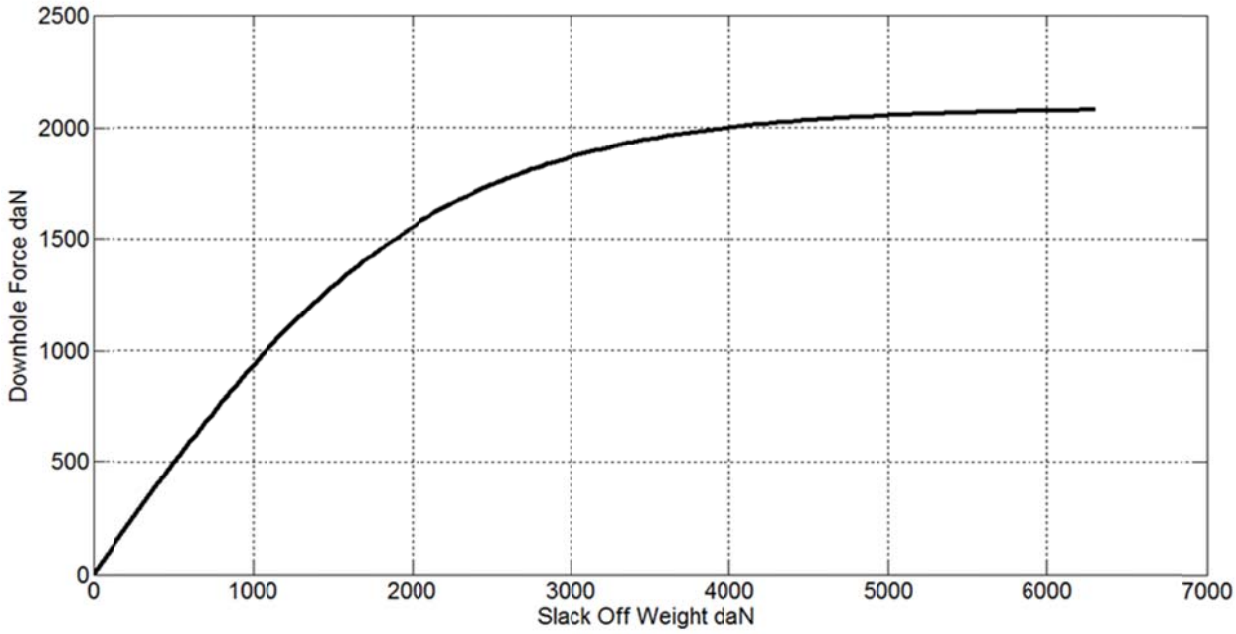

Figure 5-13: Slack off weight calculation for vertical section

Then, the CT string was run to the end of the curved section and the corresponding slack off weight calculation is shown in Figure 5-14. The lock-up condition was achieved after 144 iterations. The Addition of the results for the curved section to those for the vertical section could result in numerical artifacts in plot.

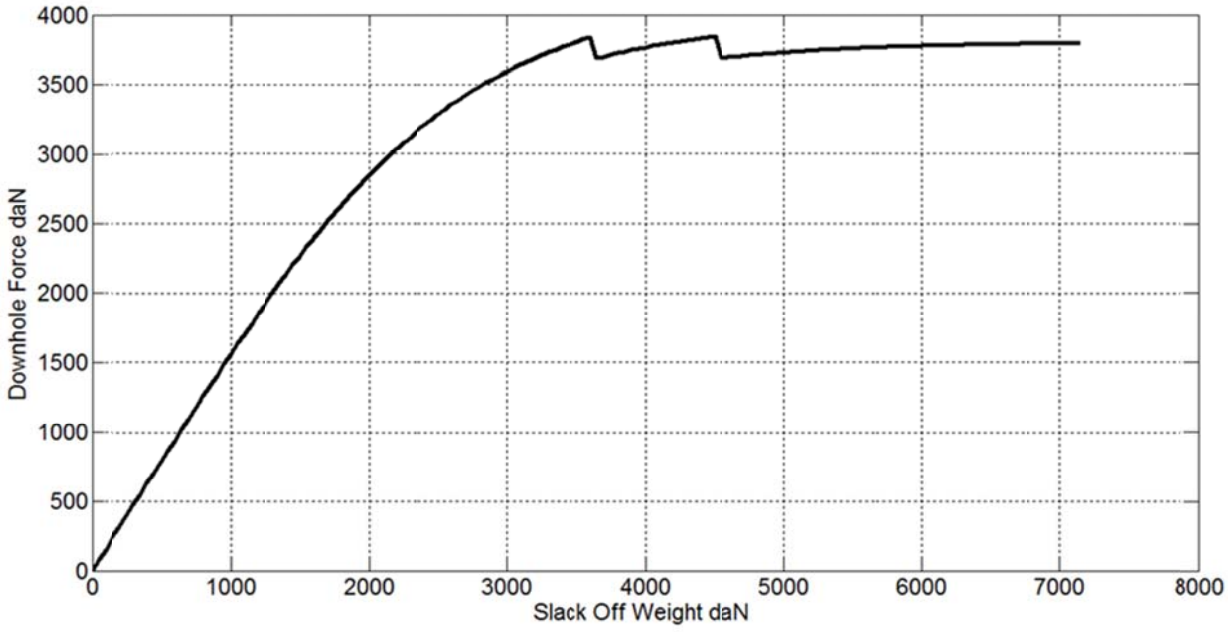

Figure 5-14: Slack off weight calculation for vertical and curved (heel) sections

Finally, the CT string was run to the end of the horizontal section at a depth of 4565.92 mMD and the corresponding slack off weight calculation is shown in Figure 5-15. The lock-up condition was achieved after 72 iterations. Again, extending the depth to include the horizontal section could result in numerical artifacts in the plot. A red dotted line is used as a visual aid to show the trend of convergence.

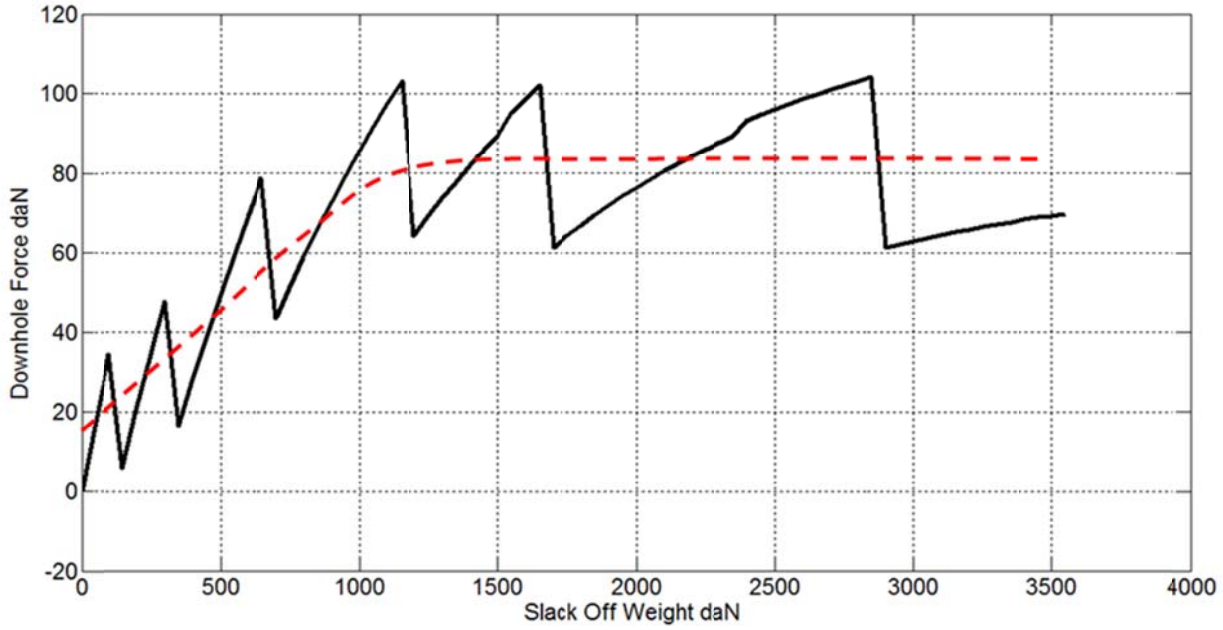

Figure 5-15: Slack off weight calculation for vertical, curved and horizontal sections

Next, a more extended depth is considered. The axial compressive force is shown in Figure 5-16 for CT string at a depth of 4584.91 mMD. The CT string was predicted to helically buckle towards the end of the vertical section and at the beginning of the horizontal section.

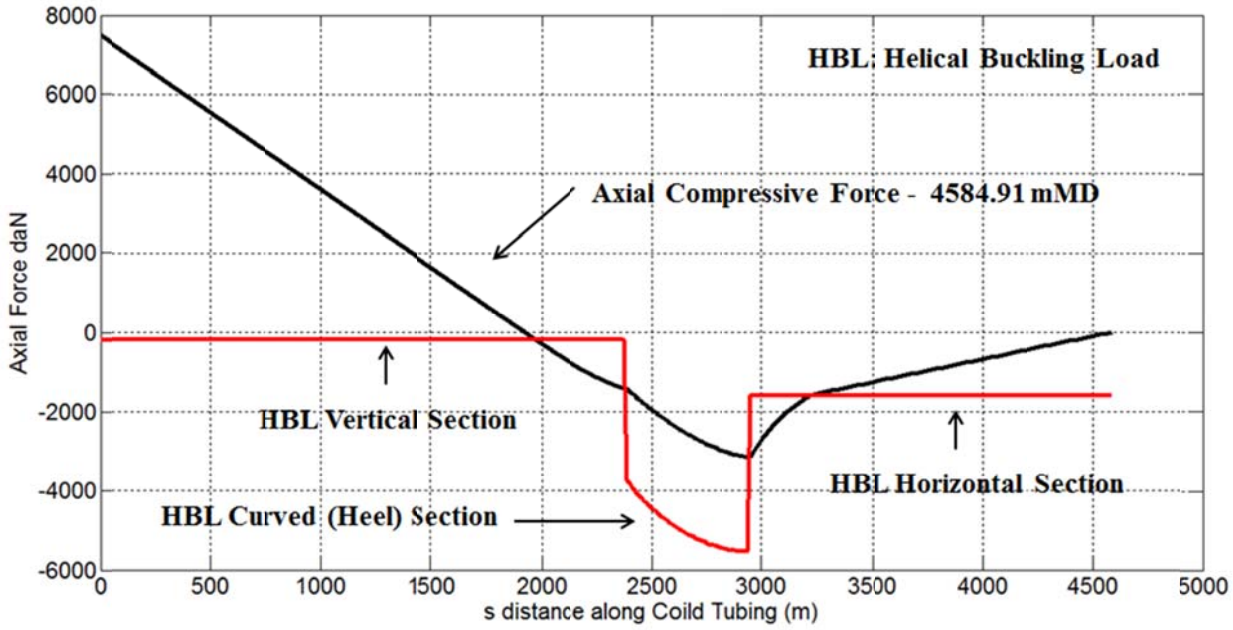

Figure 5-16: Axial Compressive force for CT string at depth of 4584.91 mMD

The plot of the slack off weight is shown in Figure 5-17. The lock-up condition is achieved after 68 iterations, which implied that the CT string can indeed reach the desired depth of 4584.91 mMD. A red dotted line is used as a visual aid to show the trend of convergence.

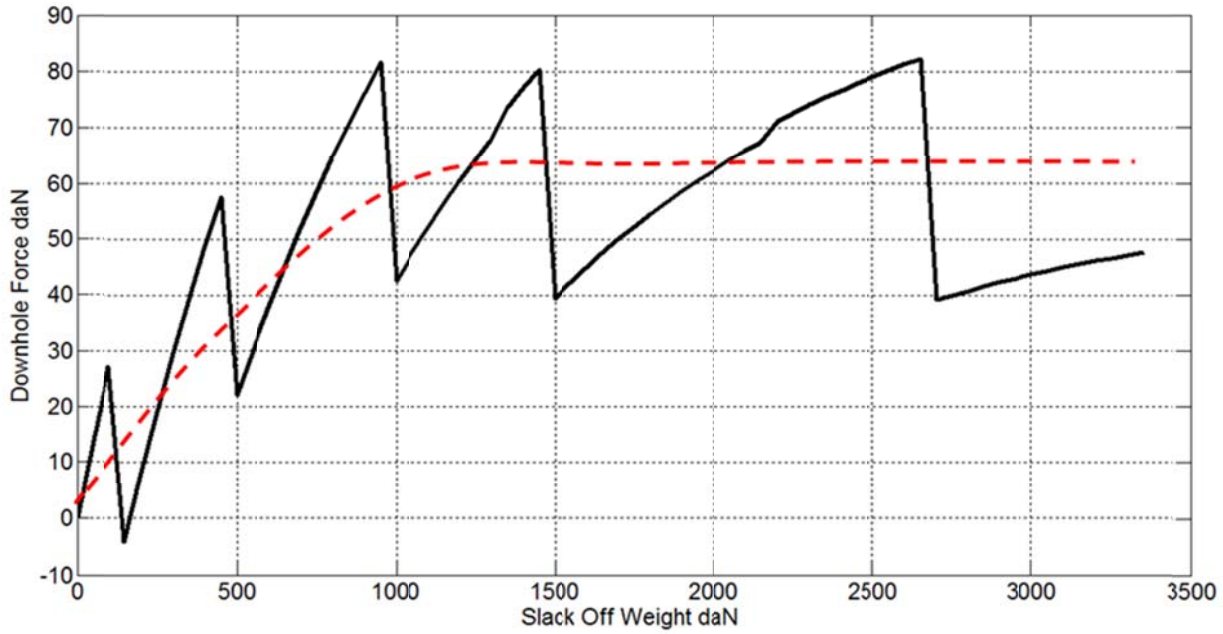

Figure 5-17: Slack off weight graph for CT string at depth of 4584.91 mMD

Figure 5-18 reports the graph of the axial compressive force for the CT string deployed at depth of 4665.92 mMD. For the case of the longer reach (4665.92 mMD), the segment of CT string that helically buckles comprises more than half of the length of the vertical section and the beginning of horizontal section. Because of the much larger portion of the vertical section of the CT that attains helical buckling, the amount of force transferred to the downhole end is drastically reduced.

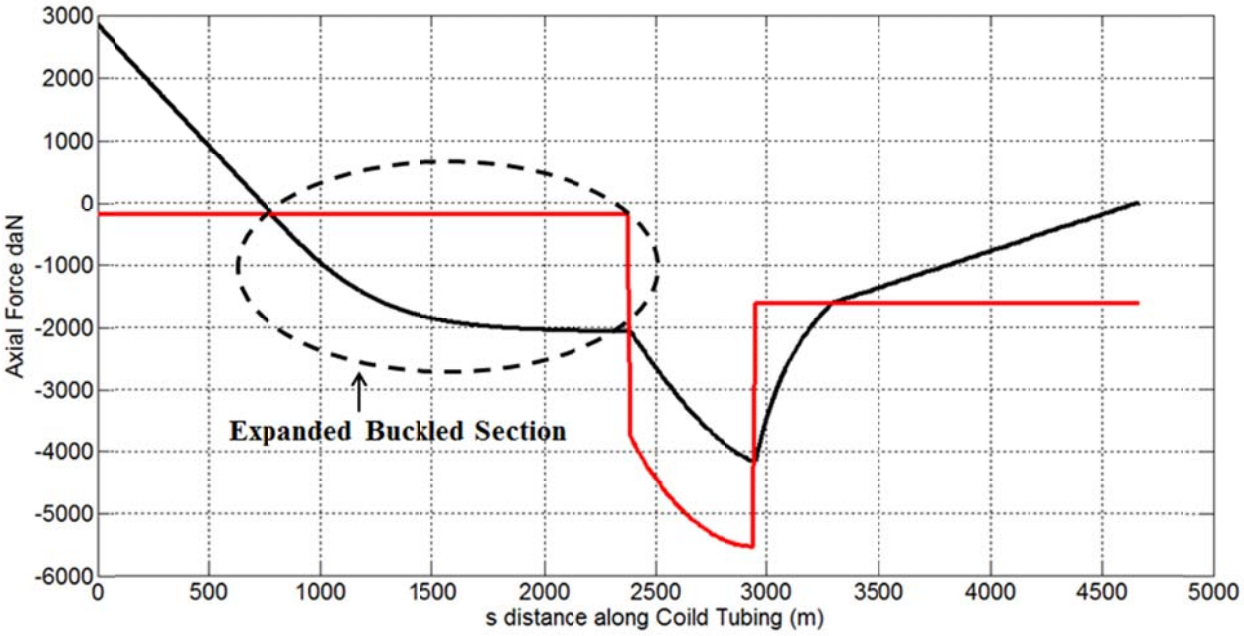

Figure 5-18: Axial Compressive force for CT string at depth of 4665.92 mMD

As it is expected from the plot of the axial compressive force (Figure 5-18), the program for the calculation of the slack off weight stops after only 6 iterations and the lock-up condition is achieved (Figure 5-19). This means that CT string cannot reach to the desired depth of 4665.92 mMD.

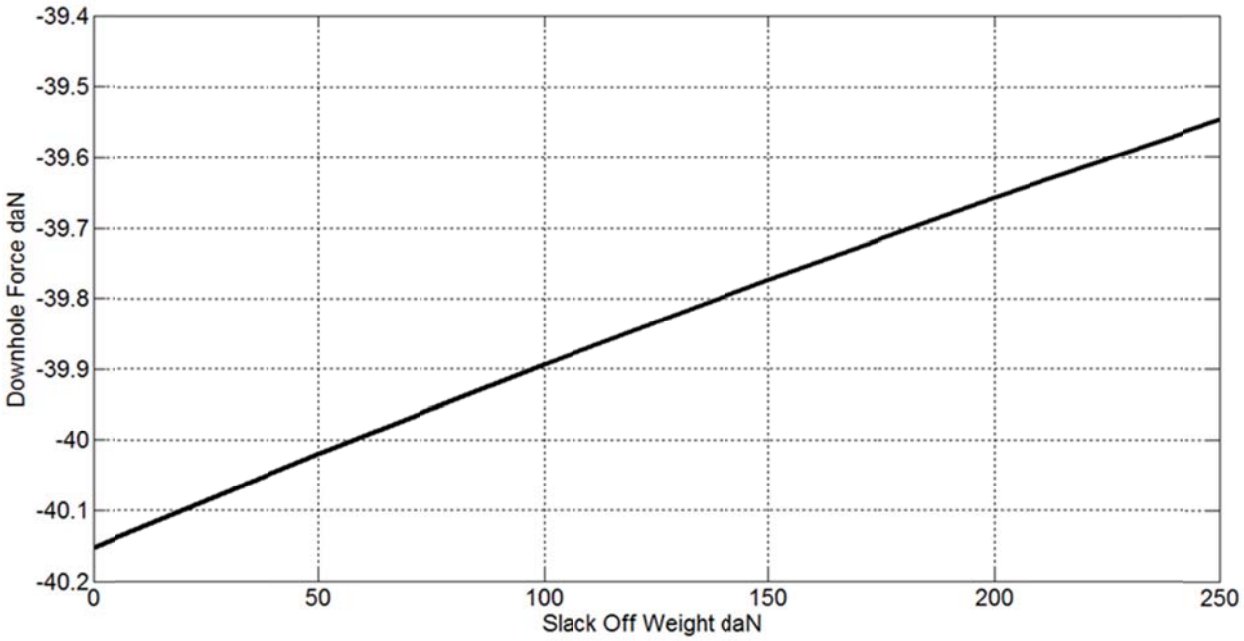

Figure 5-19: Slack off weight graph for CT string at depth of 4665.92 mMD

As mentioned above, a remedy for this problem is the application of a downhole vibrating tool (Agitator). Based on the experimental data available (Newmann, 2007A, 2007B, 2009), the application of a downhole vibrating tool results in a smaller friction force between wellbore and string, which is interpreted by means of an apparent friction factor. In order to model the effect of vibration, we use a value of 0.185 for the apparent friction factor ($\mu_{apprent\_helical}$) of the helically buckled section. In Figure 5-20, the axial compressive force is plotted for the vibrating case, showing that the downhole vibration reduced the extent of the helically buckled sections both in the vertical and the horizontal sections of well.

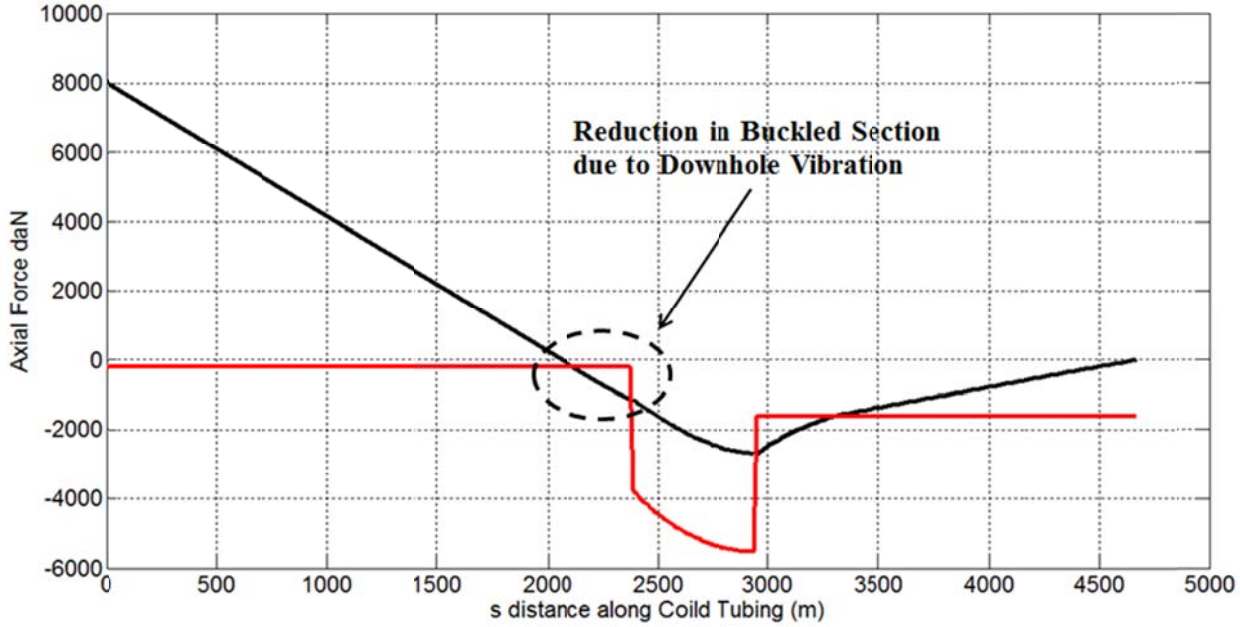

Figure 5-20: Downhole Vibration Application - Axial Compressive force at 4665.92 mMD

The calculation of the slack off weight is shown in Figure 5-21. The lock-up condition is achieved after 50 iterations, which means that the CT string can reach to the desired depth and confirms that downhole vibration is effective in extending the CT reach. A red dotted line is used as a visual aid to show the trend of convergence.

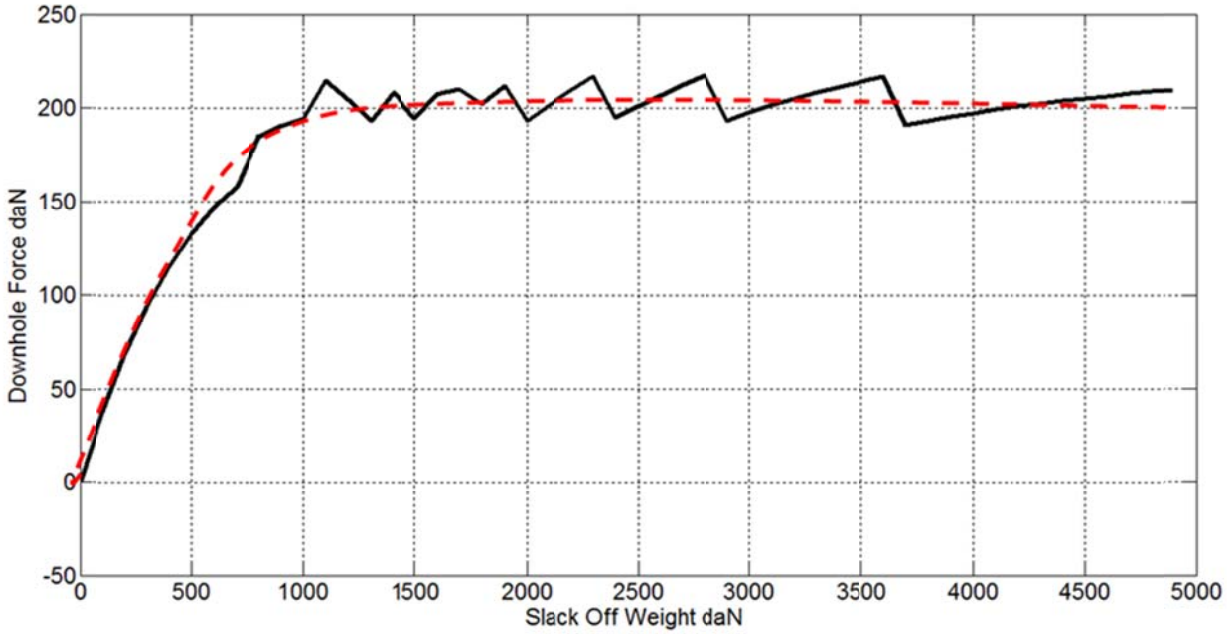

Figure 5-21: Downhole Vibration Application – Slack off weight at 4665.92 mMD

Chapter 6. Summary and Recommendations

This thesis focused on the effect of downhole vibration in enhancing load transfer and thus extending Coiled Tubing reach in a horizontal wellbore. Previous studies regarding different aspects of buckling and of the effect of downhole vibration in Coiled Tubing intervention have been reviewed in Chapter 2. In Chapter 3, we introduced: the surface equipment and downhole tools which are required to perform Coiled Tubing intervention; the different types of CT well intervention applications; the challenges and limitations which CT intervention requirements encounter during design phase and operations; and the application of downhole vibration as a remedy to these challenges. Chapter 4 introduced helical buckling load and axial load distribution relations for vertical, curved and horizontal sections of a wellbore. These relations have been extracted from the literature, as they are commonly used in the industry.

The core results of the thesis have been presented in Chapter 5. A modeling approach has been introduced to explain the effect of vibration in enhancing load transfer using the concept of apparent friction factors. The proposed model has been compared against the very limited published experimental data available (Newman et al., 2007A, 2007B, 2009). In order to show the effect of downhole vibration in extending the reach of a CT, two cases of CT intervention have been modeled, namely with and without the application of downhole vibration. The trend shows that, in the straight ad sinusoidal sections, the method of the multiple apparent friction factors shows an improvement in the implementation of the relations proposed for the buckled CT.

The effect of downhole vibration as a means to extend CT reach is a well-established method in the oil and gas industry. Surface tests confirm the improvement of load transfer as a result of vibration. A better understanding of downhole vibration in CT intervention and the proposal of a modeling approach were the main objectives of this thesis. Considering the information available in the public domain, this research was meant to add to the subject of downhole vibration by means of a simple approach, which can describe the effect of downhole vibration with a relatively small number of parameters.

Some subjects suggested as possible future research topics are

1. The design of further surface tests with actual sizes of CT strings in order to broaden the available experimental data;
2. The study of the contact force due to the effect of vibration and the validation against experimental data;
3. The development of a comprehensive vibration model for an entire wellbore.

References

Akgun, F. et al. (1996). Theoretical and Experimental Evaluation of Drill Pipe Stability Conditions in Slim Holes. Society of Petroleum Engineers. doi:10.2118/37392-MS

Apostal, M. C. et al. (1990). A Study To Determine the Effect of Damping on Finite-Element-Based, Forced-Frequency-Response Models for Bottomhole Assembly Vibration Analysis. Society of Petroleum Engineers. doi:10.2118/20458-MS

Barakat, E. R. (2005). An Experimental Study and Modeling of the Effect of Hydraulic Vibrations on Axial Force Transfer in Horizontal Wellbores. This report is prepared for TUDRP Advisory Board Meeting Nov 14-15, 2005. Tulsa-Oklahoma

Barakat, E. R. et al. (2007). The Effect of Hydraulic Vibrations on Initiation of Buckling and Axial Force Transfer for Helically Buckled Pipes at Simulated Horizontal Wellbore Conditions. Society of Petroleum Engineers. doi:10.2118/105123-MS

Bernt S Aadnøy and Ketil Andersen (2001),"Design of oil wells using analytical friction models", Journal of Petroleum Science and Engineering, Volume 32, Issue 1, 15 December 2001, Pages 53–71, doi:10.1016/S0920-4105(01)00147-4

Bhalla, K. (1994). Implementing Residual Bend in a Tubing Forces Model. Society of Petroleum Engineers. doi:10.2118/28303-MS

Cheatham, J. B. and Pattillo, P. D. (1984). Helical Postbuckling Configuration of a Weightless Column Under the Action of m Axial Load. Society of Petroleum Engineers. doi:10.2118/10854-PA

Chen, Y. C. et al. (1989). An Analysis of Tubing and Casing Buckling in Horizontal Wells. Offshore Technology Conference. doi:10.4043/6037-MS

Chen, Y. C., & Adnan, S. C. (1993). Buckling Of Pipe And Tubing Constrained Inside Inclined Wells. Offshore Technology Conference. doi:10.4043/7323-MS

Chen, Y.-C. et al. (1990). Tubing and Casing Buckling in Horizontal Wells (includes associated papers 21257 and 21308). Society of Petroleum Engineers. doi:10.2118/19176-PA

Cunha, J. C. (2003). Buckling of Tubulars Inside Wellbores: A Review on Recent Theoretical and Experimental Works. Society of Petroleum Engineers. doi:10.2118/80944-MS

Dawson, R. and Paslay, P. R. (1984). Drill Pipe Buckling in Inclined Holes. Society of Petroleum Engineers. doi:10.2118/11167-PA

Deli, G. et al. (1998). An Analysis of Helical Buckling of Long Tubulars in Horizontal Wells. Society of Petroleum Engineers. doi:10.2118/50931-MS

Duman, O. B. et al. (2001). Effect of Tool Joints on Contact Force and Axial Force Transfer in Horizontal Wellbores. Society of Petroleum Engineers. doi:10.2118/72278-MS

Gu, H. et al.(1993). Analysis of Slack-Off Force Transmitted Downhole in Coiled-Tubing Operations. Society of Petroleum Engineers. doi:10.2118/26511-MS

Guo, B. et al. (2013). How Much Can You Extend the Reach of Coiled Tubing in Horizontal Wells Using Pressure-Hammer/Pulsing Tools. Society of Petroleum Engineers. doi:10.2118/164527-MS

Hammerlindl, D. J. (1980). Packer-to-Tubing Forces for Intermediate Packers. Society of Petroleum Engineers. doi:10.2118/7552-PA

He, X., & Kyllingstad, A. (1995). Helical Buckling and Lock-Up Conditions for Coiled Tubing in Curved Wells. Society of Petroleum Engineers. doi:10.2118/25370-PA

Heisig, G., & Neubert, M. (2000). Lateral Drillstring Vibrations in Extended-Reach Wells. Society of Petroleum Engineers. doi:10.2118/59235-MS

Hishida, H. et al. (1996). Prediction of Helical / Sinusoidal Buckling. Society of Petroleum Engineers. doi:10.2118/36384-MS

Kuru, E. et al.(1999). The Buckling Behavior of Pipes and Its Influence on the Axial Force Transfer in Directional Wells. Society of Petroleum Engineers. doi:10.2118/52840-MS

Kwon, Y. W. (1988). Analysis of Helical Buckling. Society of Petroleum Engineers. doi:10.2118/14729-PA

Li, Z. (1999a). Fundamental Equations for Dynamical Analysis of Rod and Pipe String in Oil and Gas Wells. Society of Petroleum Engineers.

Li, Z. (1999b). Static Buckling of Rod and Pipe String in Oil and Gas Wells. Society of Petroleum Engineers.

Love, A. E. H., (1944). “A Treatise on the Mathematical Theory of Elasticity”, Fourth Edition, Dover Publications, New York, 1944

Lubinski, A. (1950)-A Study of the Buckling of Rotary Drilling Strings. American Petroleum Institute.

Lubinski, A. et al. (1962). Helical Buckling of Tubing Sealed in Packers. Society of Petroleum Engineers. doi:10.2118/178-PA

McCann, R. C., & Suryanarayana, P. V. R. (1994). Experimental Study Of Curvature And Frictional Effects On Buckling. Offshore Technology Conference. doi:10.4043/7568-MS

McSpadden, A., & Newman, K. (2002). Development of a Stiff-String Forces Model for Coiled Tubing. Society of Petroleum Engineers. doi:10.2118/74831-MS

Miska, S. et al. (1996). An Improved Analysis of Axial Force Along Coiled Tubing in Inclined/Horizontal Wellbores. Society of Petroleum Engineers. doi:10.2118/37056-MS

Miska, S., & Cunha, J. C. (1995). An Analysis of Helical Buckling of Tubulars Subjected to Axial and Torsional Loading in Inclined Wellbores. Society of Petroleum Engineers. doi:10.2118/29460-MS

Mitchell, R. F. (1982). Buckling Behavior of Well Tubing: The Packer Effect. Society of Petroleum Engineers. doi:10.2118/9264-PA

Mitchell, R. F. (1986a). Numerical Analysis of Helical Buckling. Society of Petroleum Engineers. doi:10.2118/14981-MS

Mitchell, R. F. (1986b), Simple Frictional Analysis of Helical Buckling of Tubing, 13064-PA SPE Journal Paper

Mitchell, R. F. (1988). New Concepts for Helical Buckling. Society of Petroleum Engineers. doi:10.2118/15470-PA

Mitchell, R. F. (1995). Pull-Through Forces in Buckled Tubing. Society of Petroleum Engineers. doi:10.2118/26510-PA

Mitchell, R. F. (1996). Comprehensive Analysis of Buckling With Friction. Society of Petroleum Engineers. doi:10.2118/29457-PA

Mitchell, R. F. (2002). New Buckling Solutions for Extended Reach Wells. Society of Petroleum Engineers. doi:10.2118/74566-MS

Mitchell, R. F. (2004). The Twist and Shear of Helically Buckled Pipe. Society of Petroleum Engineers. doi:10.2118/87894-PA

Mitchell, R. F. (2006). The Effect of Friction on Initial Buckling of Tubing and Flowlines. Society of Petroleum Engineers. doi:10.2118/99099-MS

Newman, K. et al. (2014). Extended Reach: Can We Reach Farther? Society of Petroleum Engineers. doi:10.2118/168235-MS

Newman, K. R. (2004). Finite Element Analysis of Coiled Tubing Forces. Society of Petroleum Engineers. doi:10.2118/89502-MS APA

Newman, K. R. et al. (2007, A).”Friction Reduction For Microhole CT Drilling”, Final Technical Report, DOE Award Number: DE-FC26-05NT15485.

Newman, K. R. et al. (2007, B). “Vibration and Rotation Considerations in Extending Coiled-Tubing Reach”, SPE paper 106979, SPE/ICoTA Coiled Tubing and Well Intervention Conference and Exhibition, 20-21 March, The Woodlands, Texas, U.S.A., March 2007

Newman, K. R. et al. (2009). Modeling the Affect of a Downhole Vibrator. Society of Petroleum Engineers. doi:10.2118/121752-MS

Oyedokun, O., & Schubert, J. (2014). Extending the Reach of Coiled Tubing in Directional Wells With Downhole Motors. Society of Petroleum Engineers. doi:10.2118/168240-MS

Pabon, J. A. et al. (2010). Modeling Transient Vibrations While Drilling Using a Finite Rigid Body Approach. Society of Petroleum Engineers. doi:10.2118/137754-MS

Paslay, P.R. and Bogy, D.B. (1964). The Stability of a Circular Rod Laterally Constrained to Be in Contact With an Inclined Circular Cylinder. J. Appl. Mech. 31(4), 605-610 (Dec 01, 1964) (6 pages) doi:10.1115/1.3629721

Qiu, W. (1998). Prediction of Contact Force for Drill Pipe/Coiled Tubing. Society of Petroleum Engineers. doi:10.2118/51092-MS

Qiu, W. et al. (1997). Effect of Coiled Tubing (CT) Initial Configuration on Buckling/Bending Behavior in Straight Deviated Wells. Society of Petroleum Engineers. doi:10.2118/39003-MS

Qui, W. et al.(1998). Effect of Coiled Tubing Initial Configuration on Buckling Behavior in a Hole of Constant Curvature. Society of Petroleum Engineers. doi:10.2118/46009-MS

Qui, W. et al. (1998). Drill Pipe/Coiled Tubing Buckling Analysis in a Hole of Constant Curvature. Society of Petroleum Engineers. SPE-39795-MS

Qui, W. (1999). Effect of Drill Pipe/Coiled Tubing Initial Configuration on Contact Force. Society of Petroleum Engineers. doi:10.2118/52189-MS

Salies, J. B. et al. (1994a). Experimental and Mathematical Modeling of Helical Buckling of Tubulars in Directional Wellbores. Society of Petroleum Engineers. doi:10.2118/28713-MS

Salies, J. B. et al.(1994b). Experimental and Analytical Study of Sinusoidal Buckling in Vertical Wells. Society of Petroleum Engineers. doi:10.2118/29164-MS

Sola, K.-I., & Lund, B. (2000). New Downhole Tool for Coiled Tubing Extended Reach. Society of Petroleum Engineers. doi:10.2118/60701-MS

Sorenson, K. G. and Cheatham, J. B. (1986). Post-Buckling Behavior of a Circular Rod Constrained Within a Circular Cylinder. J. Appl. Mech. 53(4), 929-934 (Dec 01, 1986) (6 pages) doi:10.1115/1.3171883

Sun, C. & Lukasiewicz, S. (2006). A new model on the buckling of a rod in tubing. Journal of Petroleum Science and Engineering, Volume 50, Issue 1, 16 January 2006, Pages 78-82, ISSN 0920-4105,

Terry, A. R. et al.(2004). Modeling Coiled Tubing Drag Forces - Small Factors Have a Big Impact. Society of Petroleum Engineers. doi:10.2118/89598-MS

Tikhonov, V. et al. (2013). Dynamic Model for Stiff String Torque and Drag. Society of Petroleum Engineers. doi:10.2118/163566-MS

Tikhonov, V. S. and Safronov, A. I.(2011). Analysis of Postbuckling Drillstring Vibrations in Rotary Drilling of Extended-Reach Wells. J. Energy Resour. Technol. 133(4), 043102 (Dec 07, 2011) (8 pages) doi:10.1115/1.4005241

Walker, B.R. and Friedman, M.B.(1977). Three-Dimensional Force and Deflection Analysis of a Variable Cross-Section Drillstring. J. Pressure Vessel Technol. 99(2), 367-373 (May 01, 1977) (7 pages) doi:10.1115/1.3454543

Wicks, N. et al.(2012). Modeling of Axial Vibrations to Allow Intervention in Extended Reach Wells. Society of Petroleum Engineers. doi:10.2118/156017-MS

Wu, J. (1995). Slack-off Load Transmission in Horizontal and Inclined Wells. Society of Petroleum Engineers. doi:10.2118/29496-MS

Wu, J., & Juvkam-Wold, H. C. (1993a). Study of Helical Buckling of Pipes in Horizontal Wells. Society of Petroleum Engineers. doi:10.2118/25503-MS

Wu, J., & Juvkam-Wold, H. C. (1993b), Helical Buckling of Pipes in Extended Reach and Horizontal Wells—Part 1: Preventing Helical Buckling, J. Energy Resour. Technol 115(3), 190-195 (Sep 01, 1993) (6 pages) doi:10.1115/1.2905992

Wu, J., & Juvkam-Wold, H. C. (1993c), Helical Buckling of Pipes in Extended Reach and Horizontal Wells—Part 2: Frictional Drag Analysis, J. Energy Resour. Technol 115(3), 196-201 (Sep 01, 1993) (6 pages) doi:10.1115/1.2905993

Wu, J., & Juvkam-Wold, H. C. (1995a). Coiled Tubing Buckling Implication in Drilling and Completing Horizontal Wells. Society of Petroleum Engineers. doi:10.2118/26336-PA

Wu, J. and Juvkam-Wold, H. C.(1995b). Buckling and Lockup of Tubulars in Inclined Wellbores. J. Energy Resource. Technol. 117(3), 208-213 (Sep 01, 1995) (6 pages) doi:10.1115/1.2835342

Wu, J. and Juvkam-Wold, H. C.(1995c). The Effect of Wellbore Curvature on Tubular Buckling and Lockup. J. Energy Resource. Technol. 117(3), 214-218 (Sep 01, 1995) (5 pages) doi:10.1115/1.2835343

Zhang, Y. L. (1989). A Study of Helical Buckling of the Compressed Portion of a Drillstring During Straight-Hole Drilling Using a Down-hole Motor. Society of Petroleum Engineers.

Appendix A Force-Pitch Relationship

In this appendix, the force-pitch relationship for a long, weightless string subjected to compressive force is reported, based on the work by Lubinski et al. (1962).

Assuming linear elasticity, the length L_c of the string subjected to compressive force F is

$$L_c = L\left(1-\frac{\sigma_a}{E}\right), \tag{A-1}$$

where σ_a is average axial stress and E is the Young's modulus.

The length of the helix L_h (measured along its axis) is

$$L_h = \frac{L_c p}{\sqrt{p^2+4\pi^2 r^2}}, \tag{A-2}$$

where p is pitch of the helix and r is the tubing-to-casing radial clearance.

The strain energy for axial compression is

$$U_c = \frac{1}{2}\frac{L}{EA_s}F_a^{\,2}, \tag{A-3}$$

where

$$F_a = F\sin\theta, \tag{A-4}$$

and

$$\sin\theta = \frac{p}{\sqrt{p^2+4\pi r^2}}. \tag{A-5}$$

Substituting A-4 and A-5 into A-3 yields

$$U_c = \frac{F^2 p^2 L}{2A_s E(p^2 + 4\pi^2 r^2)}. \tag{A-6}$$

The strain energy for bending is defined as

$$U_{bending} = \frac{1}{2} LEI\, C^2, \tag{A-7}$$

where C is the curvature of the helix, i.e.,

$$C = \frac{4\pi^2 r}{p^2 + 4\pi^2 r^2}. \tag{A-8}$$

Substitution of A-8 into A-7 yields

$$U_{bending} = \frac{8\pi^4 r^2 EIL}{(p^2 + 4\pi^2 r^2)^2}. \tag{A-9}$$

The potential energy for compressive force F is defined as

$$U_f = FL_h. \tag{A-10}$$

Substituting A-1 and A-5 into A-2 yields

$$L_h = \frac{pL}{\sqrt{p^2 + 4\pi r^2}} - \frac{LFp^2}{EA_s(p^2 + 4\pi r^2)}. \tag{A-11}$$

The total potential of the system is

$$U = U_c + U_b + U_f. \tag{A-12}$$

Substitution of A-6, A-9 and A-10 into A-12 yields

$$U = -\frac{F^2 p^2 L}{2A_s E(p^2 + 4\pi^2 r^2)} + \frac{8\pi^4 r^2 EIL}{(p^2 + 4\pi^2 r^2)^2} + \frac{FpL}{\sqrt{p^2 + 4\pi^2 r^2}}. \tag{A-13}$$

The condition of equilibrium is calculated by minimizing the total potential energy of the system with respect to the pitch of the helix, i.e.:

$$dU/dp = 0. \tag{A-14}$$

Applying condition A-14 to A-13 yields

$$\frac{p(p^2 + 4\pi^2 r^2)}{A_s E} F^2 - (p^2 + 4\pi^2 r^2)^{\frac{3}{2}} F + 8\pi^2 EIp = 0. \tag{A-15}$$

Solving for the smallest root (corresponding to the smallest total energy) in A-15 for F yields:

$$F = \frac{A_s E\sqrt{p^2 + 4\pi^2 r^2}}{2p}\left[1 - \sqrt{1 - \frac{32\pi^2 Ip^2}{A_s(p^2 + 4\pi^2 r^2)^2}}\right]. \tag{A-16}$$

Considering the ratio of the length of the string to the radial clearance between the string and the wellbore, in oil and gas applications the following assumption holds

$$p^2 >> 4\pi^2 r^2. \tag{A-17}$$

For a << 1, the first-order Taylor expansion of the square root can be used:

$$\sqrt{1-a} = 1 - (a/2). \tag{A-18}$$

Applying A-17 and A-18 to A-16 yields:

$$F = \frac{8\pi^2 EI}{p^2}. \tag{A-19}$$

Appendix B Sinusoidal Buckling Load

In this appendix, the equations for the sinusoidal buckling load are reported, based on the works by Paslay and Bogy (1964) and Dawson and Paslay (1984). The buckling initiation force for a pipe in horizontal wellbore is given by

$$F_{crit} = \frac{(1-\upsilon)^2}{(1+\upsilon)(1-2\upsilon)} EI \frac{\pi^2}{L^2}\left(n^2 + \frac{L^4 \rho A g}{n^2 \pi^4 EIr} \right). \tag{B-1}$$

The weight per unit length of pipe is

$$w = \rho A g \ . \tag{B-2}$$

Substituting B-2 and assuming the typical Poisson's ratio for steel ($\upsilon = 0.3$) yields

$$F_{crit} = EI \frac{\pi^2}{L^2} n^2 + EI \frac{\pi^2}{L^2} \frac{L^4 w}{n^2 \pi^4 EIr}, \tag{B-3}$$

which can be rearranged as

$$F_{crit} = EI \left[\frac{n\pi}{L} \right]^2 + \frac{w}{r} \left[\frac{L}{n\pi} \right]^2. \tag{B-4}$$

B-4 results from an eigenvalue problem (Paslay and Bogy, 1964) where *n* is the order of buckling that occurs in a pipe length of *L*. Considering a long pipe and treating n as a continuous variable, the minimum value of F_{crit} is obtained by imposing

$$\frac{\partial F_{crit}}{\partial n} = 0 \,. \tag{B-5}$$

Applying condition B-5 to B-4 yields

$$n^2 = \sqrt{\frac{L^4 w}{\pi^4 EIr}} \,. \tag{B-6}$$

Substituting B-6 into B-4 yields

$$F_{crit} = 2\sqrt{\frac{EIw}{r}} \,, \tag{B-7}$$

where F_{crit} is the required compressive force for the pipe to transition to the sinusoidal configuration in a horizontal wellbore.

For an inclined wellbore with inclination angle of θ, the distributed load due to the weight of the pipe, in the direction orthogonal to the pipe is

$$w = \rho Ag \sin\theta \,, \tag{B-8}$$

Replacing B-8 into B-7 yields

$$F_{crit} = 2\sqrt{\frac{EI\,\rho Ag \sin\theta}{r}} \,, \tag{B-9}$$

where F_{crit} is the required compressive force for the pipe to transition to the sinusoidal configuration in an inclined wellbore.

Appendix C Helical Buckling Load

In this appendix, the equations for the helical buckling load are reported, based on the works by Cheatham and Pattillo (1984) and Chen et al. (1989).

The strain energy for bending is defined as:

$$U_{bending} = \frac{1}{2} LEI\, C^2, \tag{C-1}$$

where C is the curvature of the helix, i.e.,

$$C = \frac{4\pi^2 r}{p^2 + 4\pi^2 r^2}. \tag{C-2}$$

Applying C-2 into C-1 yields

$$U_{bending} = \frac{8\pi^4 r^2 EIL}{(p^2 + 4\pi^2 r^2)^2}. \tag{C-3}$$

The number of full waves in a buckled pipe (m) is

$$m = \frac{L}{p}. \tag{C-4}$$

In oil and gas applications the following assumption holds

$$p^2 >> 4\pi^2 r^2. \tag{C-5}$$

Substituting C-4 and C-5 into C-3 yields

$$U_b = \frac{8\pi^4 EILr^2}{(L/m)^4}. \tag{C-6}$$

The work done by the external axial force F is:

$$W_e = F(L_c - L_z), \tag{C-7}$$

where L_c is the length of the compressed pipe prior to buckling and L_z is the length of the helix measured along its axis.

Considering the geometry of the helix, we have that

$$L_c - L_z = L - L\sin\theta, \tag{C-8}$$

and

$$\sin\theta = \frac{p}{\sqrt{p^2 + 4\pi r^2}}. \tag{C-9}$$

For a << 1, the first-order Taylor expansion of the square root can be used:

$$\sqrt{1+a} \cong 1 - (a/2). \tag{C-10}$$

Substituting C-4, C-5, C-8, C-9 and C-10 into C-7 yields

$$W_e = \frac{2FL\pi^2 r^2}{(L/m)^2}. \tag{C-11}$$

The change in potential energy when the pipe transitions from straight to helical shape, with the center of gravity at the center of the hole is

$$V = wLr, \tag{C-12}$$

where r is the radial clearance between pipe and wellbore wall.

Conservation of energy law requires

$$W_e = U_b + V . \tag{C-13}$$

Substituting C-6, C-11 and C-12 into C-13 yields

$$\frac{2FL\pi^2 r^2}{(L/m)^2} = \frac{8\pi^4 EILr^2}{(L/m)^4} + wLr . \tag{C-14}$$

Solving the C-14 with respect to F yields the helical buckling force

$$F^* = 4EI\left(\frac{m\pi}{L}\right)^2 + \frac{w}{2r}\left(\frac{L}{m\pi}\right)^2 . \tag{C-15}$$

Now, by minimizing the helical buckling force F^* with respect to number m of full waves in the buckled rod, i.e.,

$$\frac{\partial F^*}{\partial m} = 0 , \tag{C-16}$$

the value of *m* is obtained as

$$m^2 = \sqrt{\frac{w}{8rEI}}\left(\frac{L}{\pi}\right)^2 . \tag{C-17}$$

Substituting C-17 into C-15 finally yields

$$F^* = \left(2\sqrt{2}\right)\sqrt{\frac{EIw}{r}} . \tag{C-18}$$